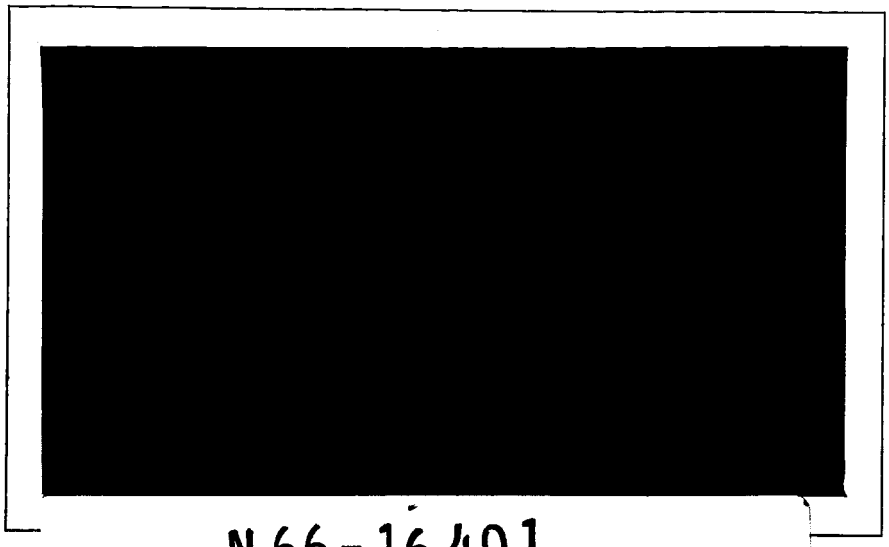

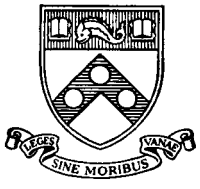

UNIVERSITY OF PENNSYLVANIA

ELECTROCHEMISTRY LABORATORY

PHILADELPHIA, PENNSYLVANIA 19104

REPORT NO. 6

QUARTERLY PROGRESS REPORT

1 JULY 1965 to 30 SEPTEMBER 1965

STUDIES IN FUNDAMENTAL CHEMISTRY OF FUEL CELL REACTIONS

NsG-325

Submitted to:

NATIONAL AERONAUTICS AND SPACE ADMINISTRATION

Washington 25, D. C.

Submitted by:

Professor John O'M. Bockris

The Electrochemistry Laboratory
The University of Pennsylvania
Philadelphia, Pa. 19104

TABLE OF CONTENTS

ABSTRACTS

Section I. The Mechanism of Various Types of High Rate Electrodes

The effect of purification on the behavior of the model porous electrode was studied. The currents observed in the pure system are about an order of magnitude higher than under impure conditions, and much more reproducible. The apparent activation effect observed in impure solutions is due to removal of impurities.

Linear current potential behavior (quasi-ohmic) is observed in the pure system as predicted previously. Most of the current is produced at the edge of the meniscus.

Section II. The Mechanism of Electrocatalysis

The work on the catalytic activity of simple electrode reactions (H_2/H^+; Fe^{+3}/Fe^{+2}) has been continued and extended to include alloys of non-noble with noble metals (Ni-Pd; Ni-Pt) and alloys of non-noble metals (Fe-Ni). Data on the hydrogen evolution reaction on a series of Pd-Ni alloys are given and briefly discussed. The alloys employed in this work were not anodically pulsed and thus the data reflect the true characteristic of the alloy composition.

Section III. The Electric Double Layer at the Solid-Solution Interface

The potential of zero charge V_{pzc} and its variation with pH have been measured on Pt. V_{pzc} decreases linearly with increasing pH with a slope of $dV_{pzc}/dpH = 2.3\ RT/F$, when measured on the normal hydrogen scale. It is independent of pH on the reversible hydrogen scale and has a value of 0.565 ± 0.025 V.

Hydrogen was very carefully eliminated from the electrodes and it was shown that the pH dependence is independent of the existence of adsorbed hydrogen, while the value of V_{pzc} at any pH depends strongly on it.

Section IV. Adsorption in the Double Layer with Special Reference to Thermal Effects

During the reporting period a new coworker was trained in the radiotracer technique of adsorption measurements, and some of the previous measurements of adsorption of benzene on Pt were reproduced. Preparations were made to initiate studies of adsorption by electrochemical methods.

Section V. Electrode Kinetic Aspects of Electrochemical Energy Conversion

Equations were derived for the terminal cell potential, differential resistance, efficiency and power of an electrochemical energy converter as a function of current drawn from the cell. To simplify the treatment, the anode and cathode were assumed to be smooth planar electrodes. Numerical calculations of these relations were carried out varying the exchange current densities, limiting current densities of the two electrodes and the ohmic resistance of the cell to examine their effects on the nature of these relations. The results are presented graphically. A brief summary of the analysis of some models which could improve electrode performance is given.

I. THE MECHANISM OF VARIOUS TYPES OF HIGH RATE ELECTRODES

In the period reported the effect of purification on the behavior of the model porous electrode was studied. A special purification train for gases as well as arrangements for extensive cleaning of the cell and purification of electrolyte by pre-electrolysis were built.

The results obtained under those pure conditions with a slit $\sim$ 5 mm wide, in the bottom, and top position of the meniscus are shown in Fig. 1.

In Table I, the results are compared with those obtained previously under non-purified conditions.

From the above comparison the following conclusions may be drawn:

1. 'Activation' of the Pt electrode is purely due to the removal of impurities by oxidation and/or desorption, since in the purified system currents are $\sim$ 10 times higher, extremely well reproducible and no hysteresis, or so-called 'activation' is observed.

2. Linear current-potential behavior observed at bottom position connected thus almost entirely with free meniscus (only $\sim$ 0.5 cm^2 of electrode is in contact with solution) agrees with the previously predicted ohmic behavior. The deviations from linearity observed below 0.25 V are ascribed to the diffusion and convection at the immersed 0.5 cm^2 of Pt.

3. Curve (2) obtained for the top position of the electrode consists of the free meniscus current and of diffusion and convection limiting currents or the additional 7 cm^2 of the electrode. By

TABLE I

	Non-purified System	Purified System
Value of current at 0.2 V	~ 0.35 mA	1.05 mA
at 1 V (top position)	~0.8 mA	3.2 mA
Reproducibility	± 50 - 100%	± 1 - 2%
Activation	If electrode exposed to potentials above ~600 mV higher currents (up to 400%), slowly decaying, in time to 'non-activate' values.	Non existent above 1%
i-V relation in steady state bottom position	Quasi linear up to 0.15 V	Almost perfectly linear over entire range (up to 1 V)
i-V relation top	No conclusions possible in comparison of top and bottom, owing to very poor reproducibility, Currents in position of top and bottom are often inverted giving less current for top position.	Closely linear. Deviations caused by contribution of additional 5 cm^2 of immersed electrode, i.e. diffusion and convection currents.

subtracting (curve 1) from curve (2) the value of this limiting current is obtained (curve 3). It is interesting to note that 7 cm^2 of Pt produces less than 1/2 of the current produced by the meniscus edge alone.

Further work will concern the current-potential relation of a

reaction with much lower exchange current than hydrogen ionization on Pt, in order to determine the effect of activation control on the model porous electrode system.

I

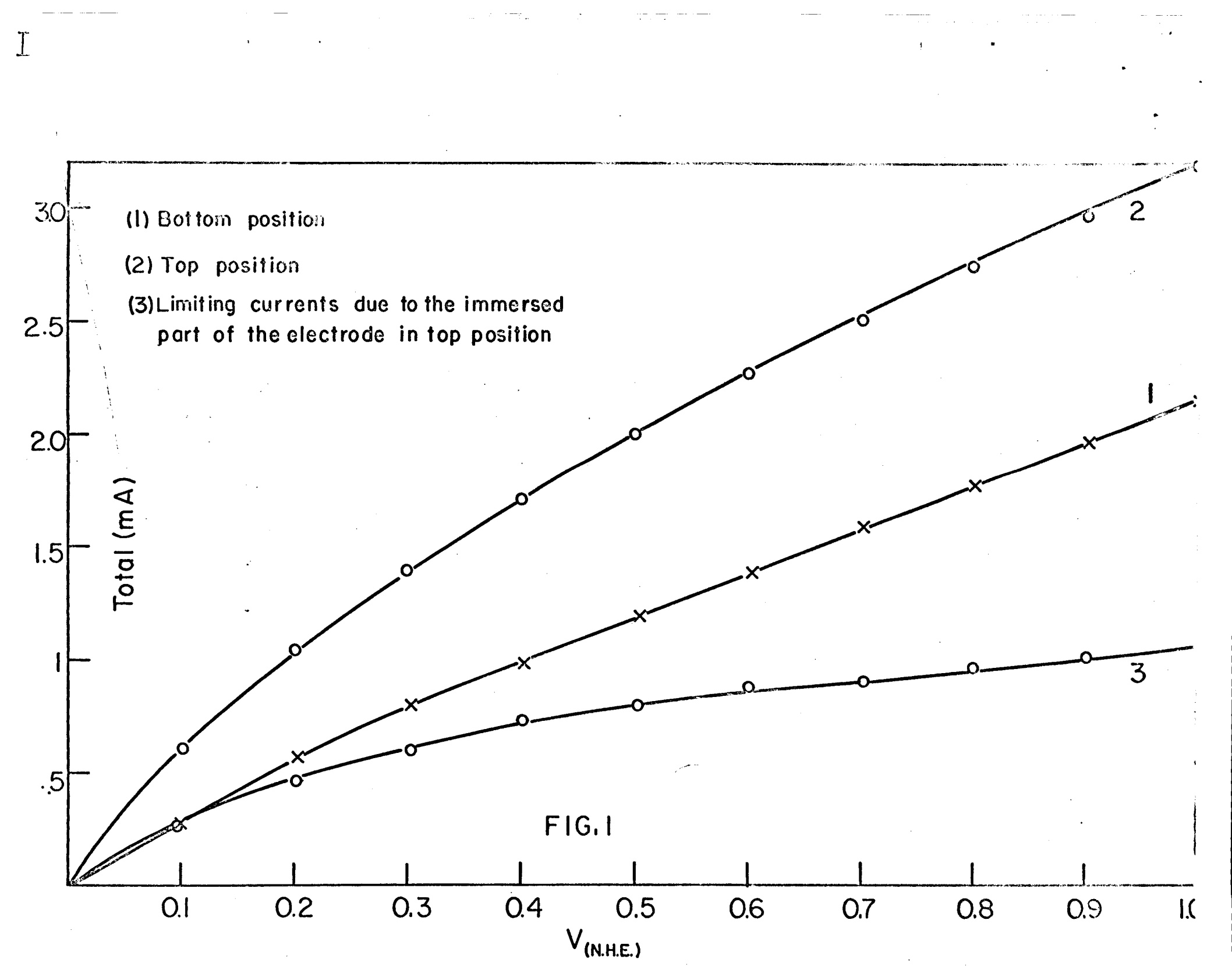
(1) Bottom position
(2) Top position
(3)Limiting currents due to the immersed part of the electrode in top position
Total (mA)
3.0
2.5
2.0
1.5
1
.5
0.1
0.2
0.3
0.4
0.5
0.6
0.7
0.8
0.9
1.0
V(N.H.E.)
1
2
3

FIG. 1

II THE MECHANISM OF ELECTROCATALYSIS

1. Introduction

The work on the catalytic activity of simple electrode reactinns, that of the H_2/H^+ and Fe^{3+}/Fe^{2+}, has been continued and extended to include other metals and alloys as electrode materials. For the purpose, alloys of non-noble with noble metals, Ni-Pd and Ni-Pt, and of non-noble non-noble metals, Fe-Ni, were made in this laboratory. Data on the H_2/H^+ reaction on a series of Pd-Ni alloys are given and briefly discussed.

2. Alloy Preparation

Pd-Ni and Pt-Ni alloys are difficult to obtain commercially in desired compositions, and were made in our laboratory. Procedure of the preparation was as follows. Weighed amount of metals (platinum, palladium and nickel) were placed in a zirconia crucible and melted in an induction furnace under purified argon atmosphere. To remove oxygen, argon was passed through a glass tube containing copper turnings and heated at 400°C. Melting lasted for a few minutes. To insure complete mixing of alloy components, an ingot after cooling to room temperature, was turned over and remelted. This procedure helped to achieve a macrohomogenous alloy. To remove coring and residual macrohomogeneity, after remelting in the induction furnace an alloy was annealed at about 1200°C for about one week. For this annealing, the alloy was placed on an alumina crucible inside a quartz tube, evacuated to 10^{-6} mm/Hg and sealed. Zirconium metal foils were placed inside the tube

and served as a getter for the residual oxygen. The quartz tube was placed inside a furnace with controlled temperature. The alloy after annealing was examined for homogeneity under an optical microscope. No indications of inhomogeneity were observed.

Initially, it was intended to work such an ingot into a wire. However, these alloys appeared to be hard and unsuitable for cold swaging.* Due to this difficulty, it was decided to mount these alloy ingots into an extended Teflon mould (Fig. 1). One side of the Teflon mould was machined to fit a true bore glass tube and to provide electrical contact. The other side was mechanically polished with emery paper (No. 4/0) and occasionally with gamal polishing solution. By the above procedure, nine alloys were made altogether. They were 3 (Pt-Ni), 3 (Pd-Ni) and 3 (Fe-Ni) alloys.

Alloy electrodes moulded in Teflon were washed with boiling CCl_4, with acetone, and then rinsed with conductivity water. They were then treated with conc. H_2SO_4 for about 30 secs. and washed thoroughly with conductivity water. Finally, they were placed in the cell and washed again with redistilled conductivity water.

From the above three alloy series, experiments have been carried out on the Pd-Ni alloys only. Further, to complete a previous analysis of Pt-Pd system,[1] one more alloy composition of Pt-Pd was examined. The experimental procedure was already described in a previous report.[2]

---

*Some Pd-Ni alloy was made into wires by alternative heating and swaging.

3. Experimental Results

The potential-log current density dependence was obtained in 1 N H_2SO_4 acid solution only in the cathodic region. Owing to the possible preferential dissolution of the less noble alloy component, the anodic side has not yet been examined. The exchange current density for the Pd-Ni alloy series varies nearly linearly with the atomic composition of the alloys (Fig. 2). The exchange current densities of the end members differ for more than two decades.

During this reporting period, further analysis of Pt-Pd system was made. It was reported previously,[1] that the mechanism of the H^+/H_2 reaction on this alloy series changes at a given alloy composition. In order to narrow the gap in the composition range over which the mechanism change occurs, one more alloy of intermediate composition was studied. In Figure 3. the 'b' parameter of Tafel relationship is plotted versus the atomic alloy composition. From this figure, it is seen that the reaction mechanism abruptly changes at about 70 at % of Pd.

4. Brief Discussion of the Results

Pd-Ni alloy series was previously examined for the same reaction in acid solution.[3] Contrary to the present experiments, it was found that activity of the electrode expressed as the exchange current density remains practically unchanged and close to that of pure Pd for most of the Pd-Ni alloys. Only the Ni electrode had a distinctly different activity from the rest of the alloys. The apparent inconsistency of these results with the present experimental data can be accounted for in

the following way. If an alloy electrode is subject to an anodic pulse for the purpose of 'activation', the less noble metal dissolves preferentially and the more noble component crystallizes over the electrode surface. In the experiments reported in the literature, Pd-Ni alloys were subject to prolonged (200 sec.) anodic pulses with a high current density (40 mA/cm^2). During such a pulse the alloy most likely becomes covered to an appreciable extent with Pd crystals. The activity for the H^+/H_2 reaction is much higher on Pd than that on pure Ni electrode. Thus higher activity results on Pd-Ni alloys. Consequently, an irregular change of activity with alloy composition was observed.

In the present experiment, the alloys were not anodically pulsed, and the data obtained reflects a true characteristic of the alloy composition.

5. Future Work

Activity for Fe^{2+}/Fe^{3+} reaction will be examined on Pt-Ni, Pd-Ni, Pt-Mo and Pt-V alloys, and for H^+/H_2 on Pt-Ni, Pt-Mo, Pt-V alloys. With the completion of the study of the above systems, the work will be extended to include compounds such as borides, nitrides and carbides of Ti. Intermetallic compounds (such as $MnAl_6$) will be studied later.

REFERENCES

1. NASA Semi-annual Progress Report, dated 1 Oct. 1964 to 30 June 1965.
2. NASA Semi-annual Progress Reprot, dated 31 Oct. 1963 to 31 March 1964.
3. Hoare, J. P. and Schuldiner, S., J. Phys. Chem., 62, 229 (1958).

LEGENDS TO FIGURES

Fig. 1 - Cross-section of Teflon holder with the alloy sample and fitted glass tube.

Fig. 2 - Change of the activity for H_2 reduction on Ni-Pd alloy electrodes in 1 N H_2SO_4 solution.

Fig. 3 - Plot of Tafel slopes versus at. % of alloy for H_2 reduction on Pt-Pd alloy series.

II

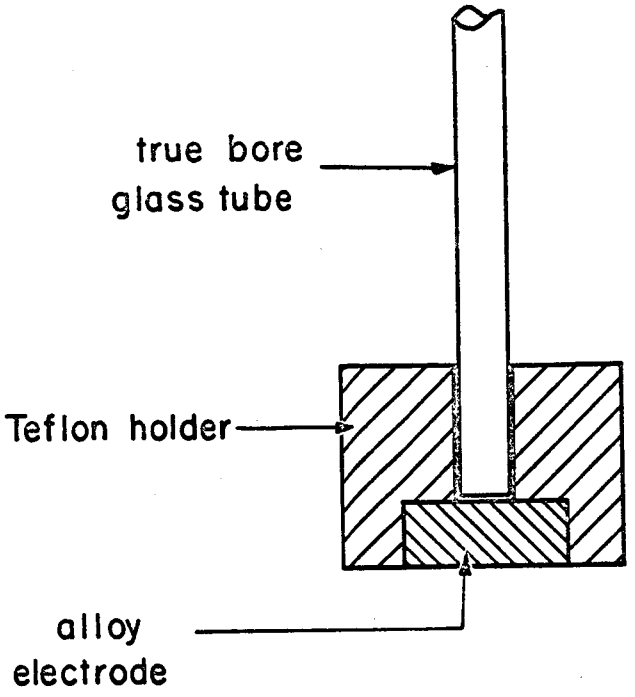

FIG. 1

II

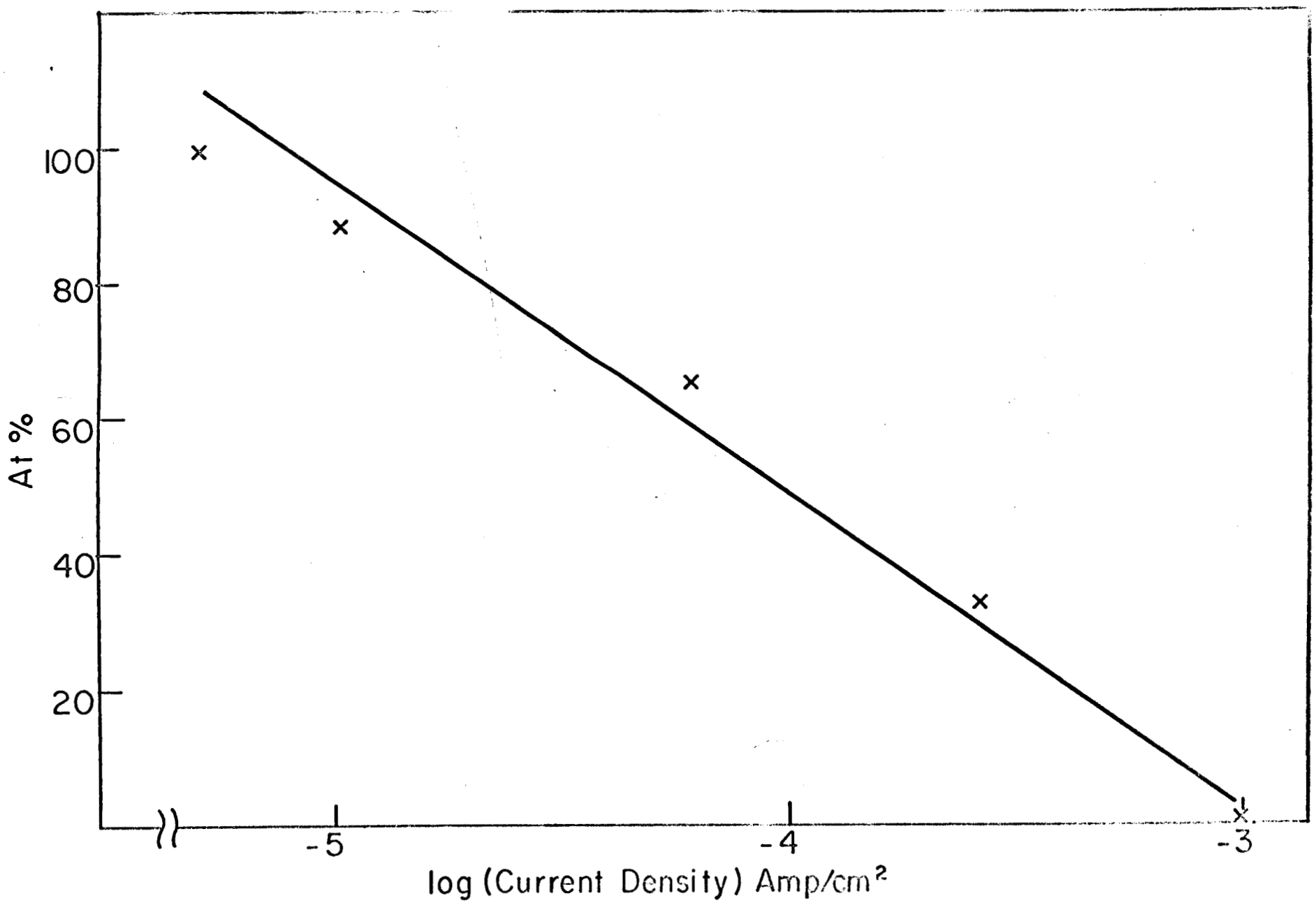

FIG. 2

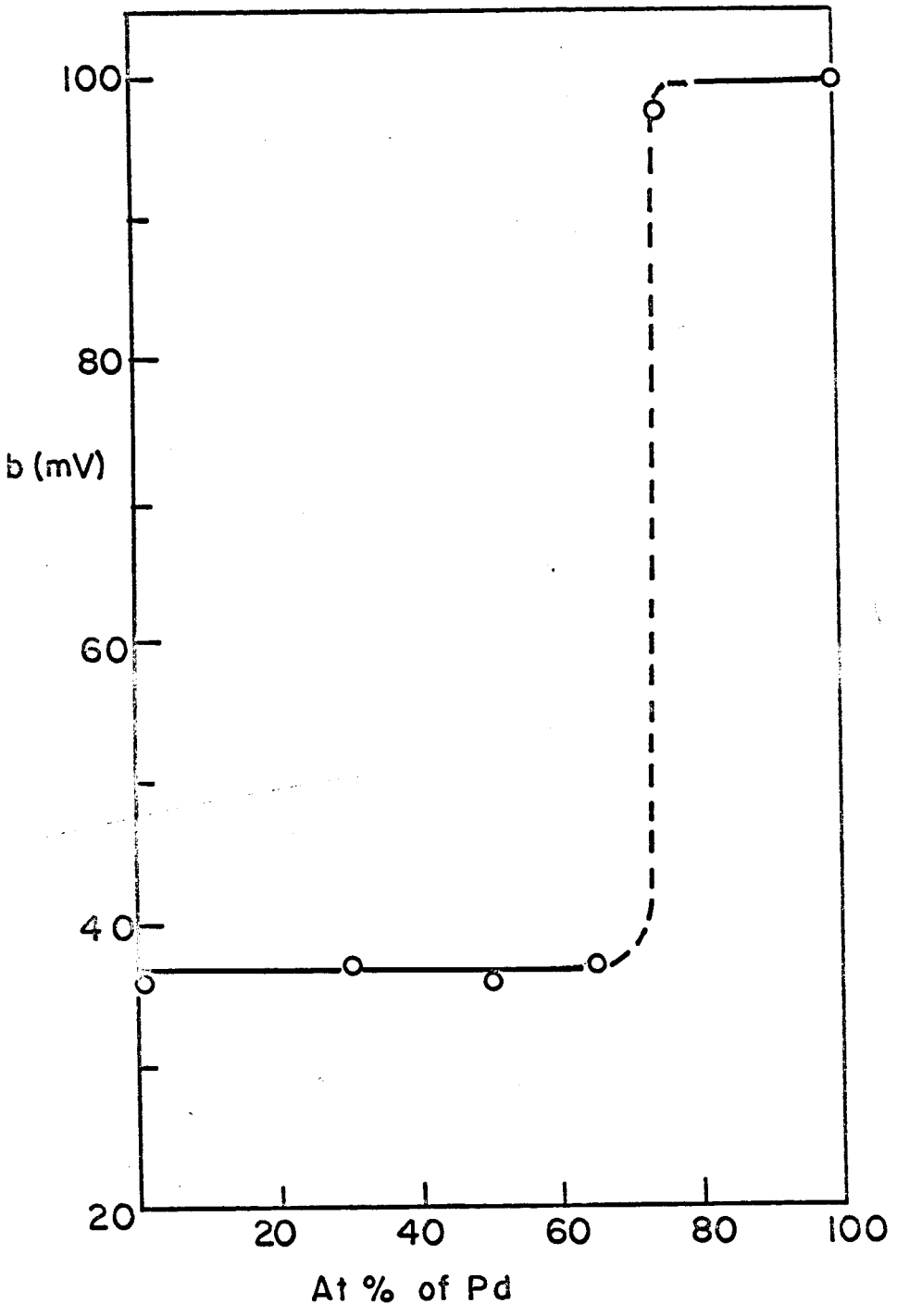

FIG. 3

III. THE ELECTRIC DOUBLE LAYER AT THE SOLID-SOLUTION INTERFACE

1. Introduction

In the report period an examination of the pH-dependence of the potential of zero charge of platinum has been made by using the differential capacitance method. In addition, the adsorption-ionic strength variation method, previously used for the determination of potential of zero charge was further confirmed using existing experimental adsorption data on mercury.

2. Experimental

The apparatus used is described in the previous report.[1] In the preparation of the electrodes 0.2 mm diameter wire was sealed into a glass tubing by means of a Housekeeper seal. This thinner tubing was joined to a long ($\sim$ 3 ft.) 'true-bore' tubing. The platinum was of spectroscopically pure quality. The thin platinum wire was surrounded by fused glass wall (1/2 mm - 1 mm diameter). The rest of the wire was melted in H_2-O_2 flame into a fine spherical ball touching the glass capillary. The bead and the glass tubing were cleaned in HNO_3 - H_2SO_4 (1 : 3) mixture, washed in distilled and double distilled water successively. The bead was introduced in a 'Vycor' furnace which was made to fit on top of the cell. The bead was heated in an argon atmosphere (99.9975% pure further purified by passing over Cu filing heated to 400°C and subsequently over molecular sieves cooled down to - 78°C) for about 1 hour. All the moisture from the glass was driven off. Then hydrogen

(purified by passing through heated Ag-Pd alloy tube) was passed at a small and steady rate for 5 minutes to remove the surface oxides. Argon was passed again for a period of 2 - 3 hours at an elevated temperature of 450°C. The furnace and the electrode were cooled down in the argon atmosphere. Few drops of mercury were put in the tubing in order to make electrical contact with the bead by means of a coaxial cable.

The solutions were purified very carefully. The reagents used were of 'analyzed reagent' grade. The double-distilled water was redistilled under a nitrogen atmosphere. ('Prepurified nitrogen' was passed over heated copper filings, silica gel and three traps cooled down to - 78°C. One of the traps was empty and the other two filled with activated charcoal which was reactivated quite often heating at 400 - 450°C under a steady stream of pure argon.) The required amounts of the reagents, perchloric acid, sodium hydroxide and sodium perchlorate were added from respective stock solutions. The total ionic strength was kept constant. The solutions were pre-electrolyzed for a minimum of 72 hours with the help of very large platinized platinum electrode (150 cm^2 geometrical area) and another smaller electrode. The pre-electrolysis was carried out at $\sim 1 \mu A/cm^2$ current density. The volume of the solution pre-electrolyzed at one time was $\sim$500 ml.

Cleaning of the glassware was done as follows. The cells were filled with warm nitric acid: sulfuric acid (1 : 3) mixture and were kept overnight. Subsequently they were washed with distilled water and double distilled water. The glassware was steamed and finally filled with distilled double-distilled water under N_2 atmosphere and were kept filled up to the time of experiment.

3. Results and Discussion

It has been reported[2] in the literature that the potential of zero charge of platinum varies with pH, because the amount of hydrogen absorbed and/or adsorbed changed with pH. It is known that the work function of platinum changes with absorption of hydrogen.[3] This in itself is one effect which will change the potential of zero charge. Therefore, it seemed necessary to investigate whether the potential of zero charge of platinum devoid of hydrogen varied with pH. The electrodes were prepared in a cautious manner to eliminate hydrogen dissolved in the electrode. The electrode was heated in argon for 1 hour and in hydrogen for 5 - 7 minutes at 350°C. The temperature was then raised to 450°C and the electrode was heated in an argon atmosphere for three hours. In this way any hydrogen which may have permeated into the bulk of the electrode was eliminated. The electrode in the solution was kept at a potential $\geq$ 450 mV R.H.E. So that coverage by atomic hydrogen was maintained at a negligible level and hydrogen absorption in the metal could not occur. The solutions were highly purified and were saturated with nitrogen. The electrode potential was changed in 25 mV steps between 400 mV and 650 mV. If the potential of the electrode was not made anodic to + 650 mV (R.H.E.) and cathodic to + 400 mV (R.H.E.) no hysteresis of capacitance was observed. If the electrode was taken to, say, + 200 mV (R.H.E.) and then the capacitance values measured as a function of potential, usually the capacitance increased and the potential of zero charge determined as the minimum of capacitance, shifted decidedly to a more negative potential, e.g., see Figures 1 and 3. Figures 1 to 7 represent the

capacitance-potential plots for the pH values of 2.5, 2.8, 3.3, 4.1, 8.0, 10.3 and 11.2 respectively. The potential refers to the reversible hydrogen electrode. The scale is purposely chosen to show that on this scale the potential of zero charge of platinum remains fairly constant. Fig. 8 shows capacitance potential plot at two frequencies. Increasing the frequency from 1000 to 2000 c/sec. affects the absolute values of the capacity in the neighborhood of the potential of zero charge but does not alter the position of the minimum on the potential scale. Table 1 shows the potential of zero charge on the reversible hydrogen scale and the normal hydrogen scale as a function of pH for electrodes from which hydrogen has been carefully eliminated. Fig. 9 shows the pH dependence of potential of zero charge on the normal hydrogen scale. It is a straight line having a slope of about 2.3 RT/F.* This is in good agreement with the assumption of Bockris, Wroblowa and Piersma.[4] Also, a recent study on adsorption of benzene on platinum as a function of pH, showed that the adsorption maximum also shifts with pH in a similar fashion.[5] Bockris, Wroblowa and Piersma have given a possible explanation of this type of behavior. According to these authors specific adsorption of hydroxyl ions, obeying a logarithmic adsorption isotherm gives the 60 mV shift of potential of zero charge per pH unit.

Fig. 10 shows the adsorption of phenol on mercury as a function of potential at various ionic strengths while keeping the concentration

---

*The p.z.c. values obtained previously by the adsorption method at pH 3 and 12 are given here for comparison. While the absolute values obtained in this manner are somewhat higher, the average variation of the potential of zero charge with pH is essentially the same.

of phenol constant at 10^{-3} M. The data was taken from Blomgren, Bockris and Jesch.[6] The intersection of the three curves is seen to be within 20 mV of each other. The individual potentials of zero charge of Hg in the respective solutions, as measured by the electrocapillary method, are shown by vertical arrows. The intersection of adsorption curves for 0.1 N HCl and 0.03 N HCl is at - 235 mV (N.H.E.). The potential of zero charge of Hg in 0.03 N HCl determined by the electrocapillary method is - 0.21 v (N.H.E.) and that for 0.1 N HCl is - 0.24 v (N.H.E.). Similarly, the intersection of 0.1 N HCl curves and 1 N HCl is at - 0.260 v (N.H.E.). The potential of zero charge of Hg for the 1 N HCl is - 0.300 v (N.H.E.). Considerable specific adsorption is involved in this case but even then the adsorption method proposed by Dahms and Green[7] for the determination of potential of zero charge gives fairly good values of the potential of zero charge. This is the first direct verification of this method. Table 2 shows the potentials of zero charge by the two methods.

4. Future work

Work is in progress for the measurement of the potential of zero charge of gold. After this work, silver and nickel will be studied in all details.

For the next method, the apparatus will be built, so as to be able to measure the coefficients of friction as a function of potential for the various systems so far studied.

TABLE 1

POTENTIAL OF ZERO CHARGE OF PLATINUM ON REVERSIBLE HYDROGEN AND NORMAL HYDROGEN SCALES AS A FUNCTION OF pH

pH	P.Z.C. on reversible hydrogen scale	P.Z.C. on normal hydrogen scale
2.5	+ 620	+ 470
2.8	+ 575	+ 407
3.3	+ 560	+ 362
4.1	+ 575	+ 329
8.0	+ 550	+ 75
10.3	+ 525	- 93
11.2	+ 550	- 122

TABLE 2

P.Z.C.'s OF Hg AS OBTAINED BY DAHMS AND GREEN METHOD AND BY THE ELECTROCAPILLARY METHOD (cf. FIG. 13)

Intersection of	P.Z.C. (N.H.E.)	Concentration	P.Z.C. (electrocapillary) (N.H.E.)
1 N and 0.1 N curves	- 0.260 V	1 N	- 0.300 V
0.1 N and 0.03N curves	- 0.230 V	0.1 N	- 0.240 V
		0.03 N	- 0.210 V

REFERENCES

1. Progress report for the period 1 Oct. 1964 to June 30, 1965 Contract NSG-325.

2. Krasikov and Kheifets: Doklady. Akad. Nauk. SSSR, 109 586 (1956).

3. Oatley: Proc. Roy. Soc. (London) 51, 318 (1939).

4. Bockris, Wroblowa and Piersma: J. Electroanal. Chem. 6, 401 (1963).

5. Heiland, Gileadi and Bockris: to be published.

6. Blomgren, Bockris and Jesch: J. Phys. Chem. 65, 2000 (1961).

7. Dahms and Green: J. Electrochem. Soc., 110, 1075 (1963).

CAPTIONS TO FIGURES

Fig. 1: Capacitance in μF cm^{-2} (geometric) plotted as a function of potential (R.H.E.) in mV in an $HClO_4$ solution of pH = 2.5 on platinum. The curve in triangles is for an electrode which was kept at + 200 for a few minutes and therefore, with hydrogen. The curve in squares is for platinum without hydrogen.

Fig. 2: Capacitance in μFcm^{-2} (geometric) plotted as a function of potential (R.H.E.) in mV in an $HClO_4$ solution of pH = 2.8 on platinum.

Fig. 3: Capacitance in μF cm^{-2} (geometric) plotted as a function of potential (R.H.E.) in mV in an $NaClO_4$ solution of pH = 4.1, on platinum. Circles are for going anodic in potential and crosses are that for going cathodic in potential , filled circles for platinum with hydrogen.

Fig. 4: Capacitance in μF cm^{-2} plotted as a function of potential (R.H.E.) in mV on platinum in a 2.8 x 10^{-3} M sodium perchlorate solution adjusted to pH = 4.1.

Fig. 5: Capacitance in μF cm^{-2} plotted as a function of potential (R.H.E.) in mV on platinum in a 3 x 10^{-3} M sodium perchlorate solution adjusted to pH = 8.

Fig. 6: Capacitance in μF cm^{-2} plotted as a function of potential (R.H.E.) in mV on platinum in a 2.9 x 10^{-3} M sodium perchlorate solution of pH = 10.2. Curve in circles is for platinum without hydrogen and the one in dots is for platinum with hydrogen.

Fig. 7: Capacitance in μF cm^{-2} as a function of potential (R.H.E.) mV on platinum in a 2 x 10^{-3} M sodium perchlorate solution of pH = 11.2. The lower curves, crosses (going cathodic) and circles (going anodic) are for platinum without hydrogen. The upper curve in circles is for platinum with hydrogen.

Fig. 8: Capacitance in μF cm^{-2} versus potential (R.H.E.) in mV on platinum as a function of frequency solution 3 x 10^{-3} M sodium perchlorate pH = 8. Triangles: 2000 cps. Circles: 1000 cps.

Fig. 9: Potential of zero charge of platinum as determined from the minimum of capacitance as a function of pH.

Fig.10: Plot of surface concentration of phenol on mercury from a bulk concentration of 10^{-3} M, varying the hydrochloric acid concentration circles 0.1 N HCl, crosses 0.03 N HCl and squares for 1 N HCl.

III

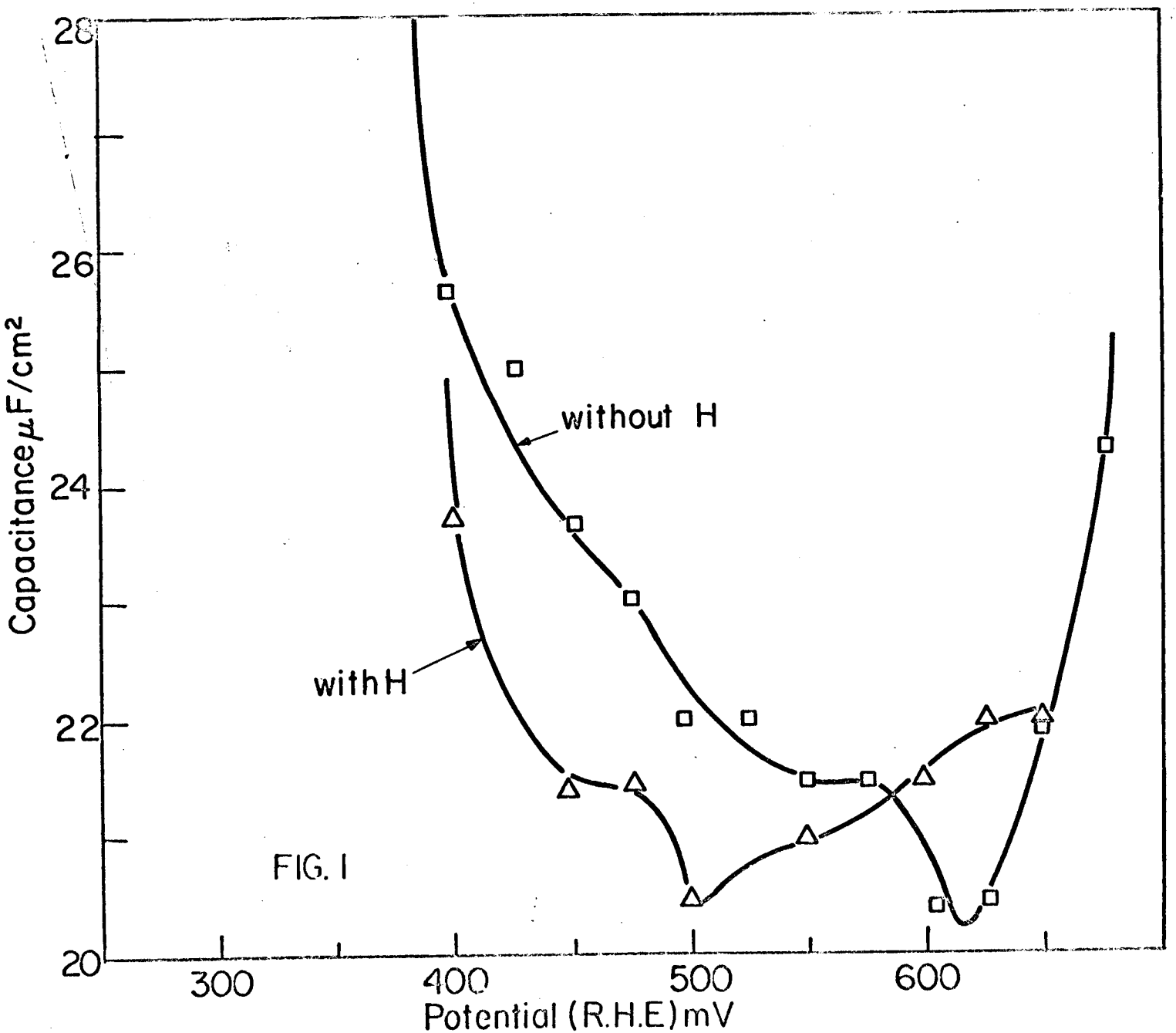
28
26
24
22
20
Capacitance μF/cm²
without H
with H
300
400
500
600
Potential (R.H.E) mV

FIG. 1

III

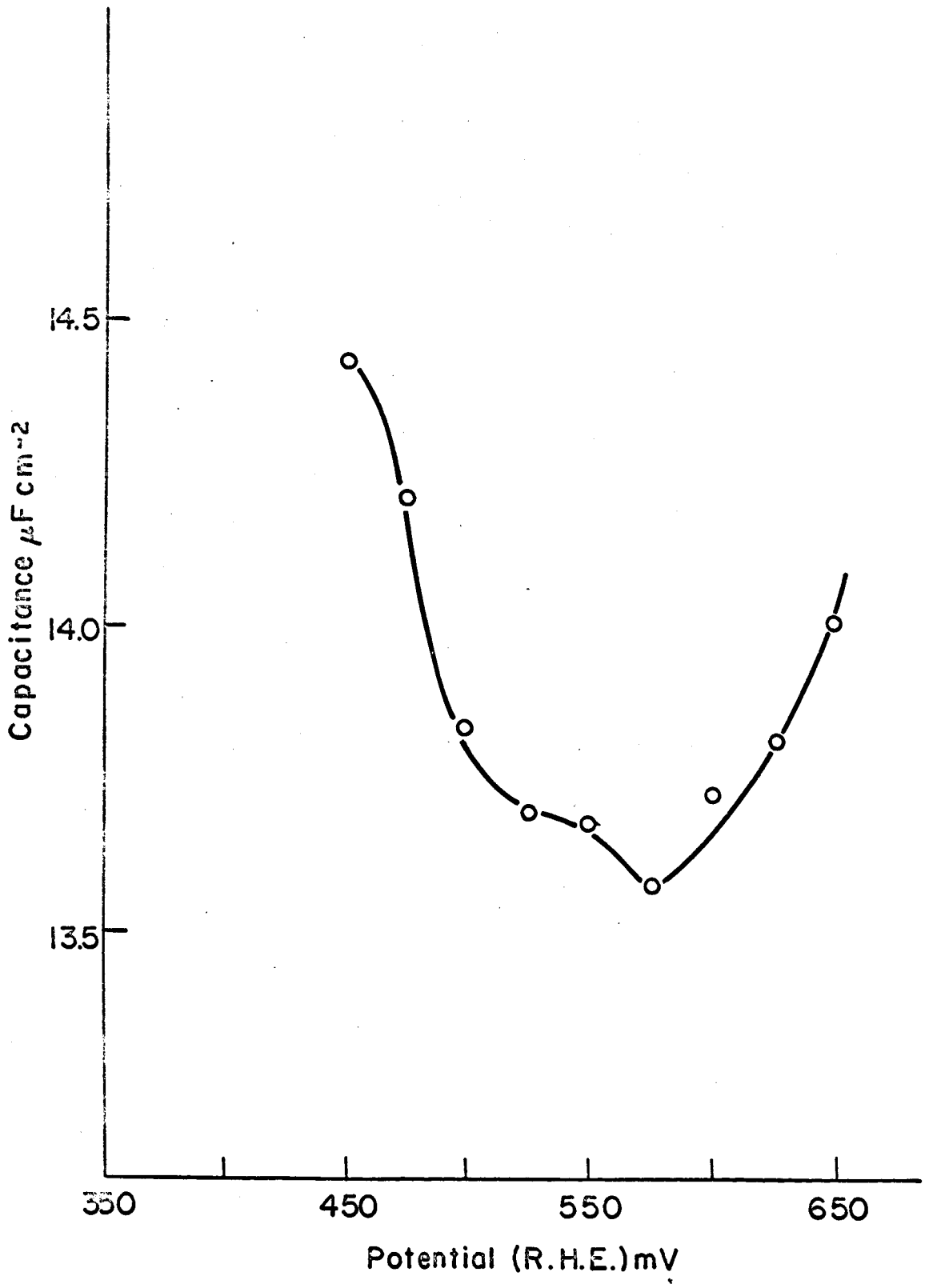
14.5
14.0
13.5
Capacitance μF cm⁻²
350
450
550
650
Potential (R.H.E.) mV

FIG.2

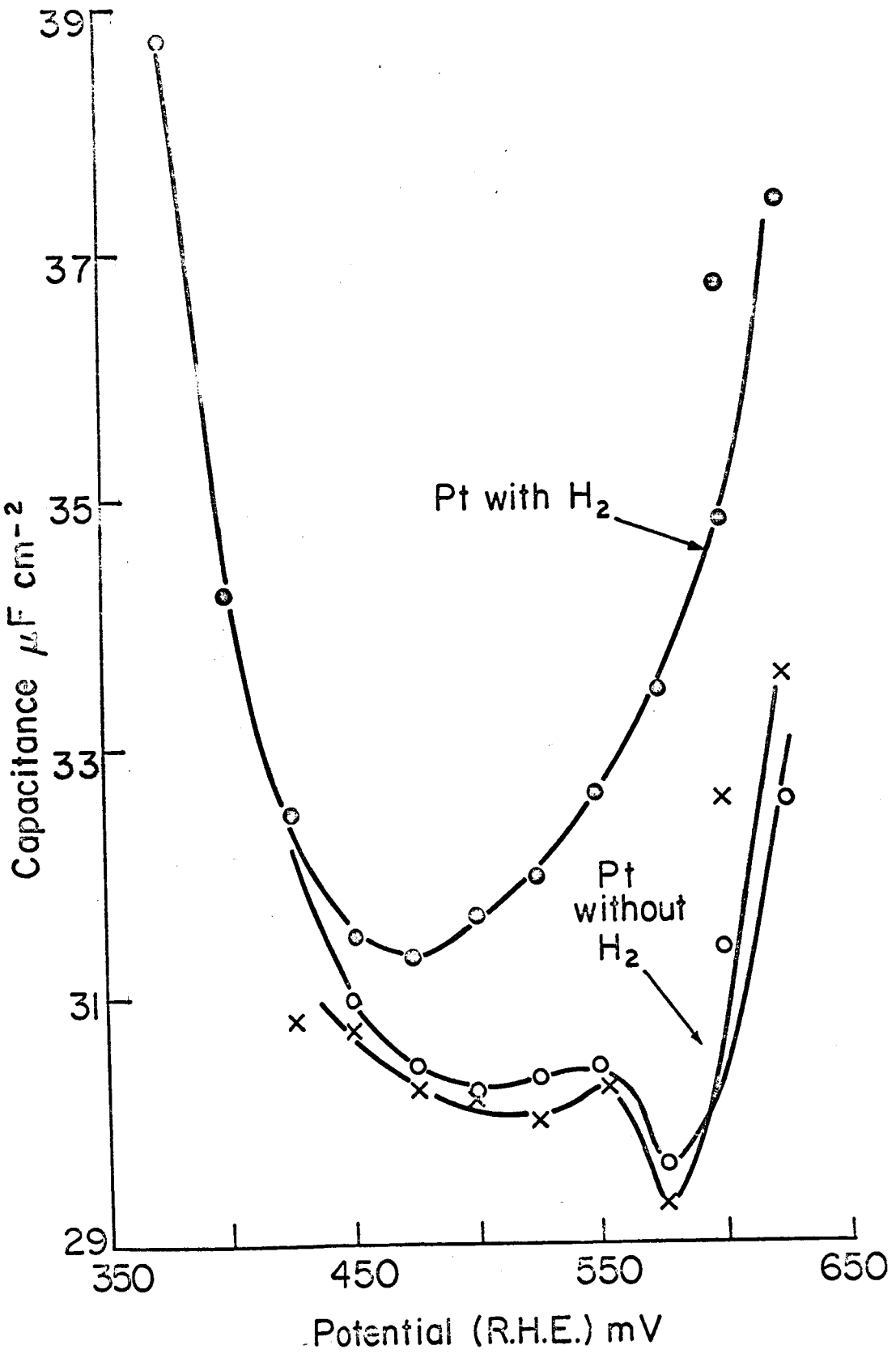
39
37
35
33
31
29
Capacitance μF cm⁻²
Pt with H₂
Pt without H₂
350
450
550
650
Potential (R.H.E.) mV

FIG. 3

III

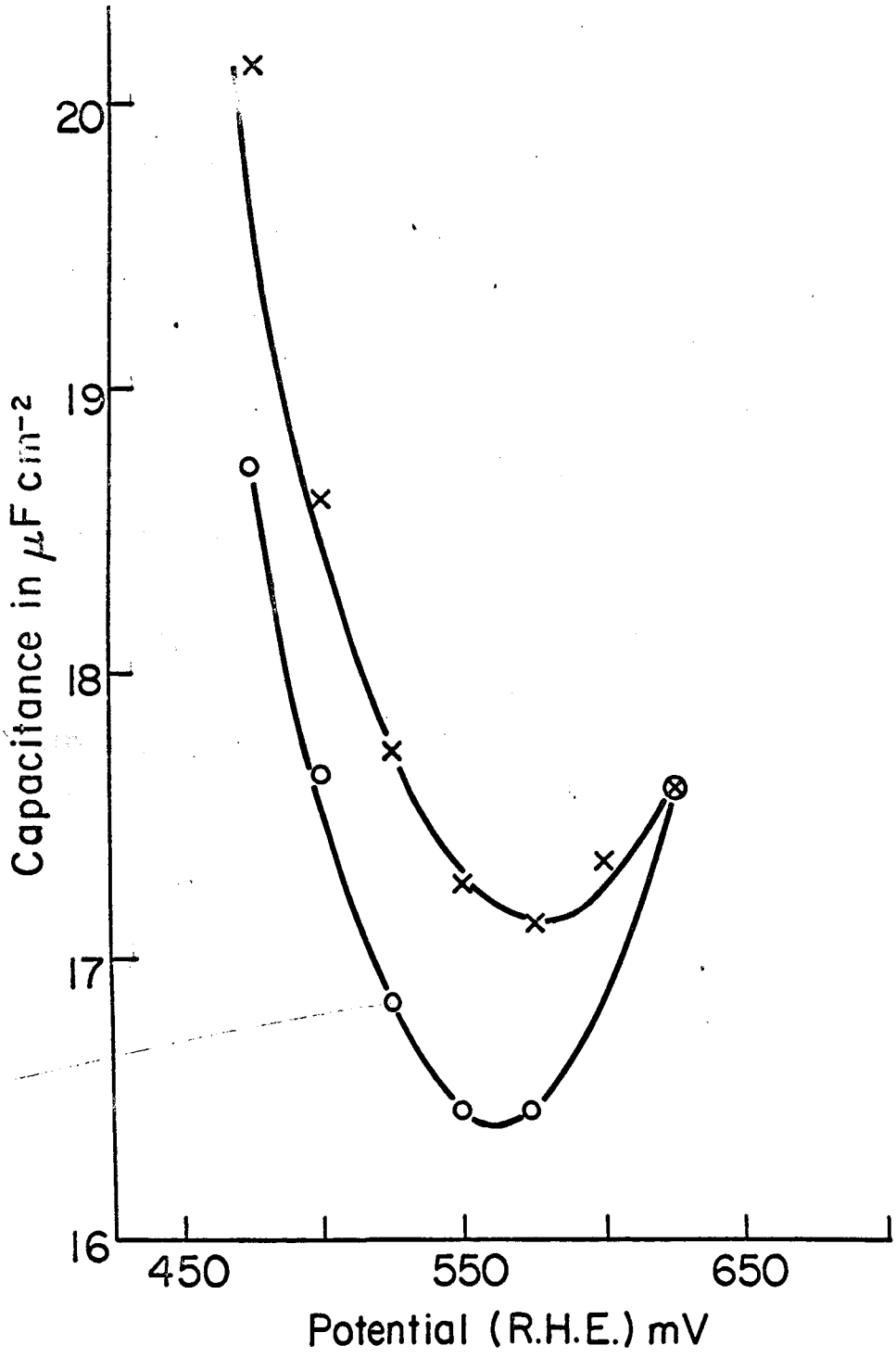
20
19
18
17
16
Capacitance in μF cm⁻²
450
550
650
Potential (R.H.E.) mV

FIG.4

III

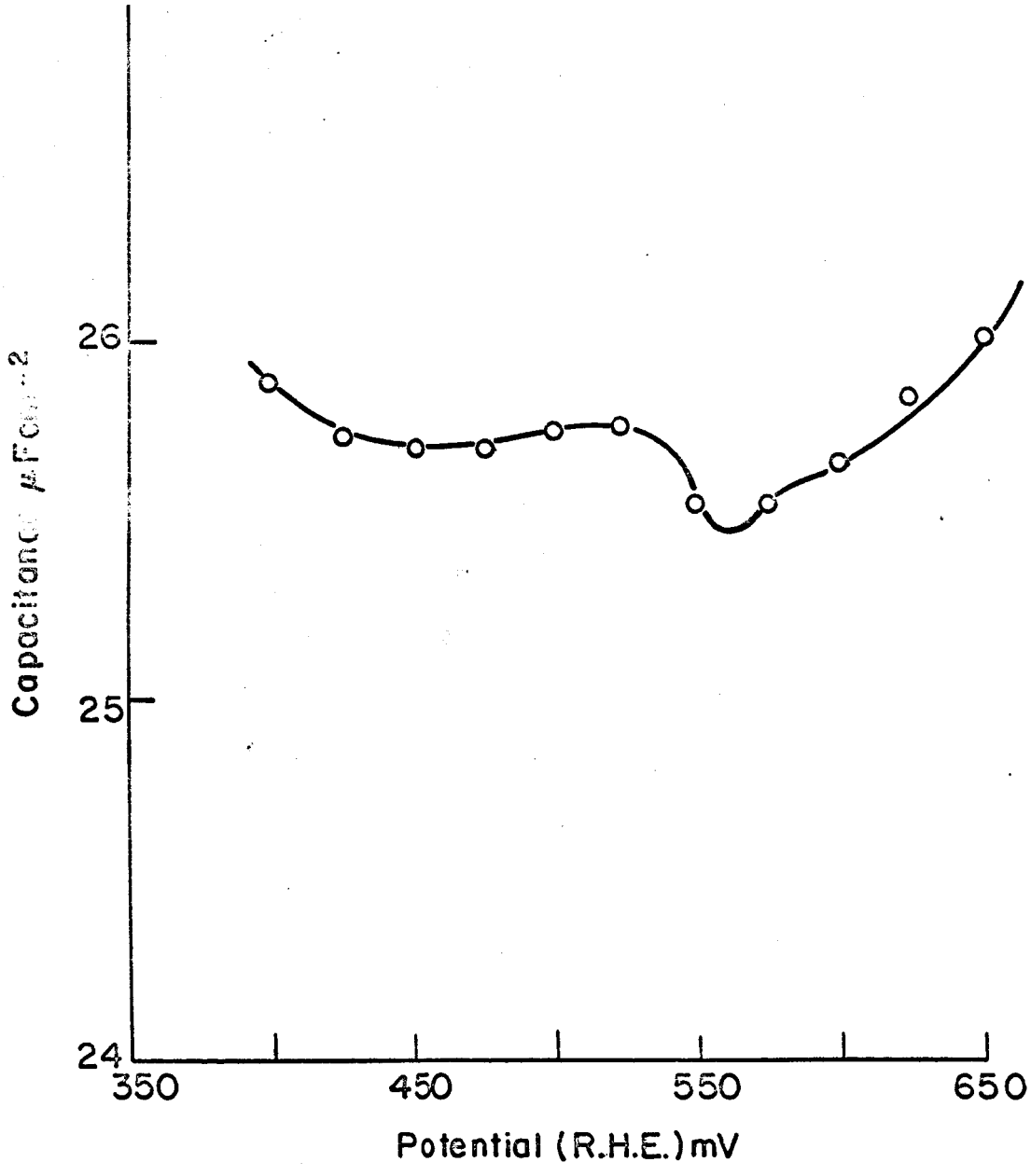

FIG.5

III

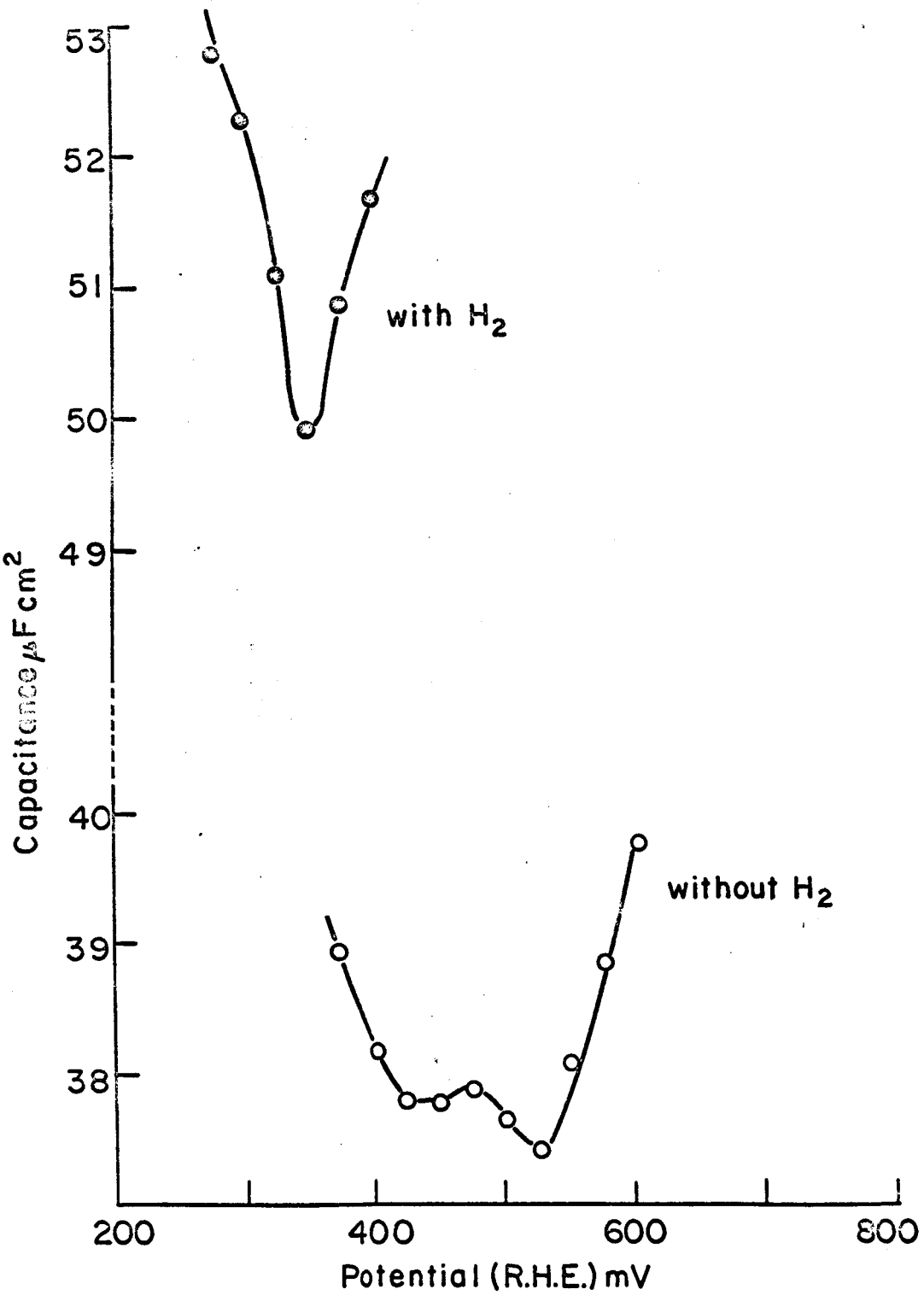
53
52
51
50
49
40
39
38
Capacitance μF cm²
with H₂
without H₂
200
400
600
800
Potential (R.H.E.) mV

FIG.6

III

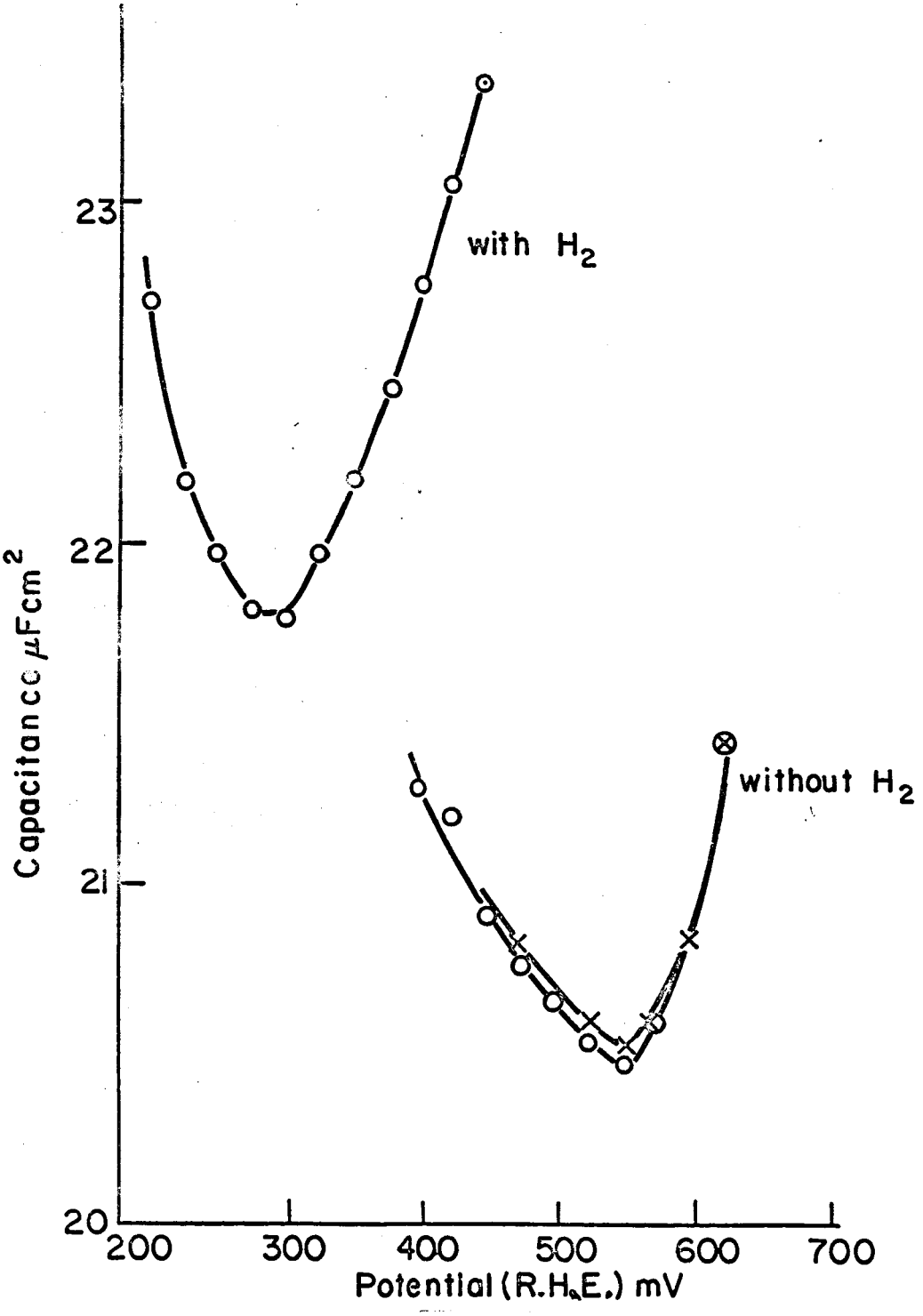
23
22
21
20
Capacitance μFcm²
with H₂
without H₂
200
300
400
500
600
700
Potential (R.H.E.) mV

FIG.7

III

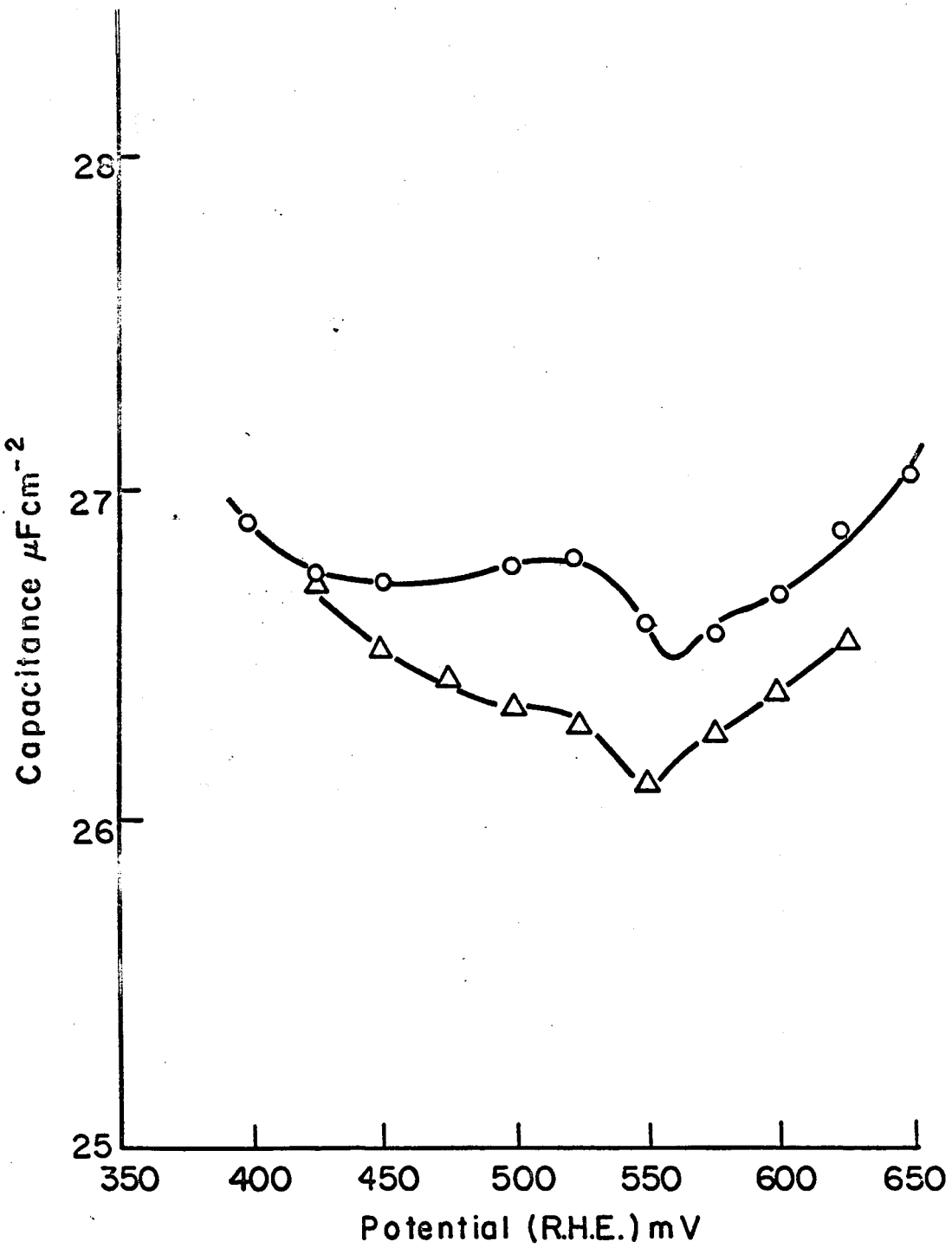
28
27
26
25
Capacitance μFcm⁻²
350
400
450
500
550
600
650
Potential (R.H.E.) mV

FIG. 8

III

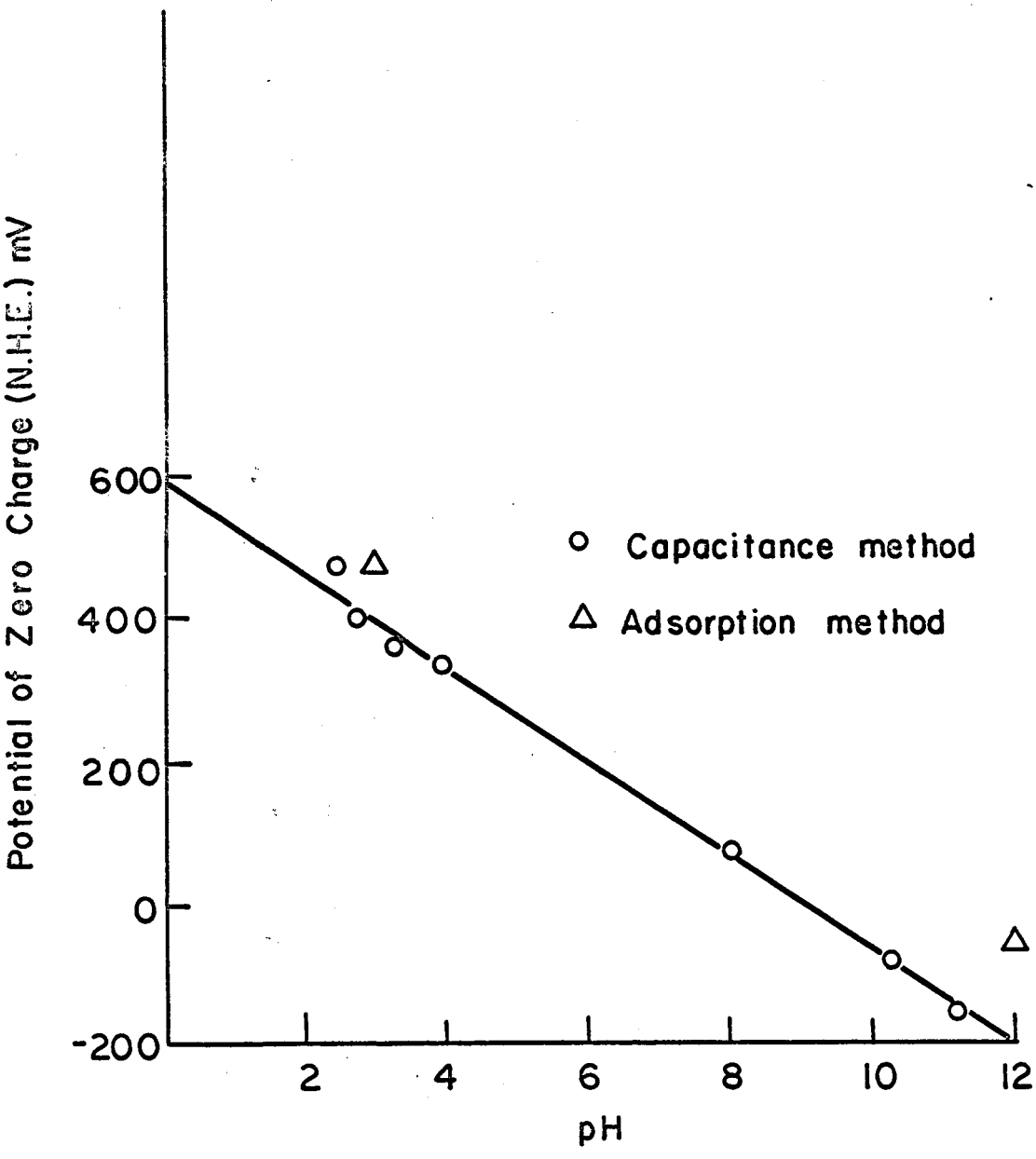
Potential of Zero Charge (N.H.E.) mV
600
400
200
0
-200
2
4
6
8
10
12
pH
Capacitance method
Adsorption method

FIG.9

III

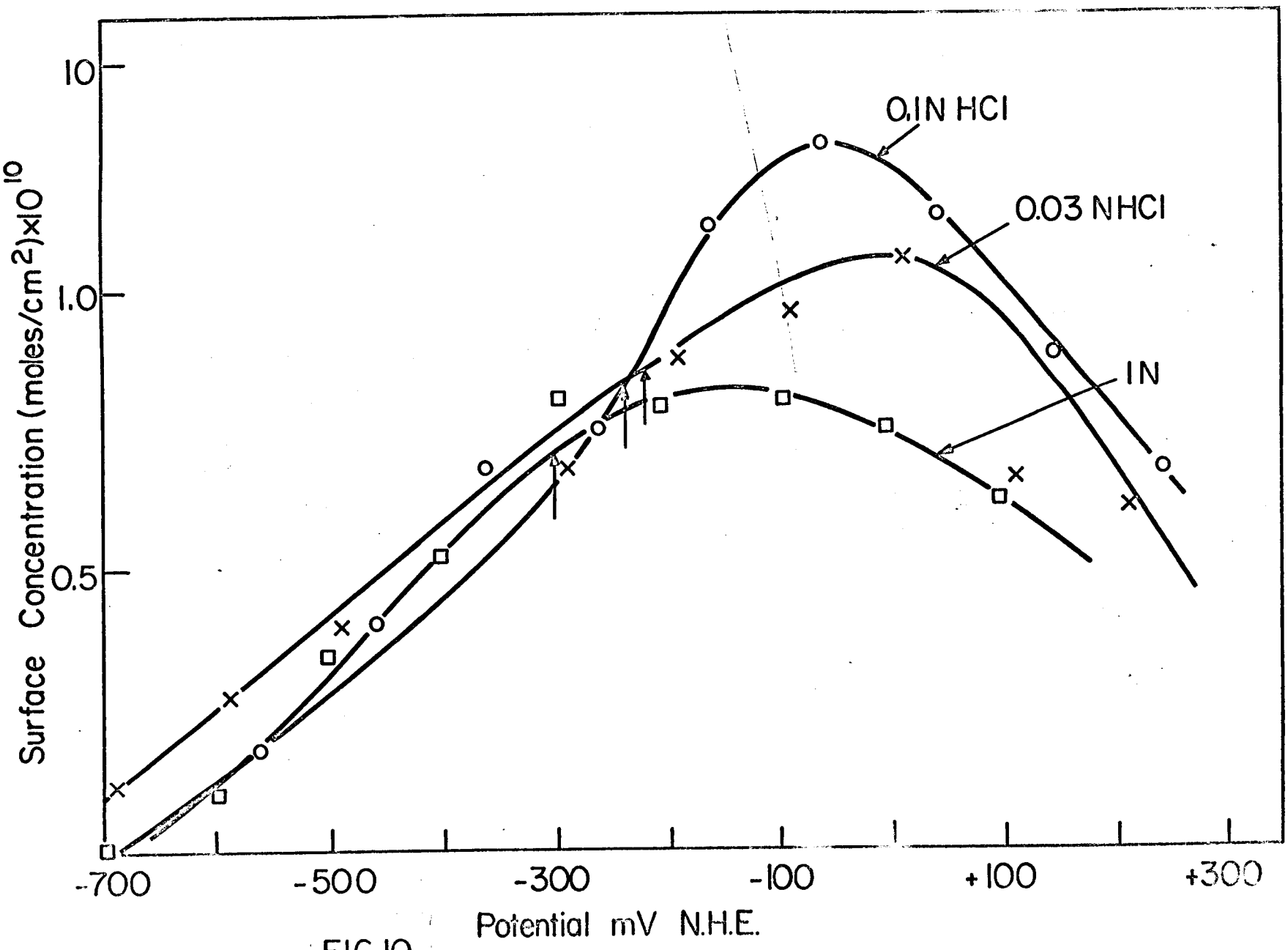
10
1.0
0.5
Surface Concentration (moles/cm²)x10¹⁰
0.1N HCl
0.03 NHCl
1N
-700
-500
-300
-100
+100
+300
Potential mV N.H.E.

FIG. 10

IV ADSORPTION IN THE DOUBLE LAYER WITH SPECIAL REFERENCE TO THERMAL EFFECTS

This project involves the study of adsorption on a number of solid electrodes (e.g., Pt, Ni, Ag) and on mercury. Specifically the adsorption of hydrogen, oxygen and, e.g., hydrozine will be tested. For studies of adsorption on mercury the electrocapillary method will be used. For adsorption on solids a radiotracer method developed in this laboratory will be used. This method involves measurement of the radiation penetrating through a thin metal foil placed over the end of an end-window proportional counter. The metal foil serves as the test electrode and is placed in an electrolytic cell which contains suitable counter and reference electrodes and a radioactively tagged adsorbate.

During the reporting period a new coworker was trained in the use of the adsorption apparatus, and previous results on the adsorption of benzene on platinum were reproduced.

In the next reporting period measurements of adsorption will be made by the radiotracer method and critically compared with several electrochemical methods used in other laboratories for the measurement of adsorption on solid electrodes.

V THEORETICAL INVESTIGATION

ELECTRODE KINETIC ASPECTS OF ELECTROCHEMICAL ENERGY CONVERSION

1. Introduction

Essentially, three types of electrochemical devices may be considered. They are the fuel cell, the driven cell and the secondary battery. The similarities and differences of the three devices are presented in Table I.

Considerable overvoltage losses exist in nearly all working fuel cells. These losses may be broadly classified under activation, mass transfer and ohmic polarization, which are the central topics in the field of electrochemical energy conversion. The following sections deal with

(1) equations for the terminal cell potential, differential resistance, efficiency and power as a function of current drawn from a fuel cell; (ii) the results of calculations carried out to examine the effect of different degrees of activation, mass transfer and ohmic polarization on the above relations; (iii) a brief summary of the analysis of some proposed models which may improve electrode performance.

2. Important electrode kinetic relations for an electrochemical energy converter

The terminal cell potential-current relation for a cell is

$$E = IR_e$$

$$= \left[E_r - \frac{RT}{\alpha_c F} \ln \frac{I}{A_c i_{o,c}} + \frac{RT}{\eta F} \ln \left(1 - \frac{I}{A_c i_{L,c}}\right) - \frac{RT}{\alpha_a F} \ln \frac{I}{A_a i_{o,a}} + \frac{RT}{\eta F} \ln \left(1 - \frac{I}{A_a i_{L,a}}\right) - IR_i \right] \qquad (1)$$

where E_r is the thermodynamic reversible potential of the cell and is given by

$$E_r = e_{r,c} - e_{r,a} \tag{2}$$

i_o, i_L, and α, with the appropriate suffices, are the exchange current density, limiting current density and the transfer coefficient of the anodic or cathodic reaction: η is the number of electrons transferred from the cathode to the anode externally, during one act of the overall reaction in the cell; and A_c and A_a are the active areas of the anode and cathode respectively.

The differential resistance of a cell is defined by

$$\frac{dE}{dI} - R_e = - \frac{RT}{\alpha_c FI} - \frac{RT}{\alpha_a FI} - \frac{RT}{\eta F(A_c i_{L,c} - I)} - \frac{RT}{\eta F(A_a i_{L,a} - I)} - R_i \tag{3}$$

The efficiency of energy conversion ($\mathcal{E}_o$) is given by

$$\mathcal{E}_o = - \frac{\eta F}{\Delta H^o} \cdot E \tag{4}$$

By substituting for E from equation (1) in (4), the efficiency-current relation is obtained. It is clear that the efficiency varies with current in the same way as does the terminal cell potential.

The power of an electrochemical energy converter is defined by the equation

$$P = EI \tag{5}$$

Using equation (1) for E in equation (5), the power-current relation for a cell is obtained.

From this general P-I relation, it is not possible to obtain analytic expressions for the maximum power and for the current density

and terminal cell potential at this maximum power level. However, such expressions may be obtained in some limiting cases.

Case (i) Conditions under which E-I relation is linear.

For this case, the terminal cell potential may be given by

$$E = E_r - R_t I \tag{6}$$

where $R_t = \frac{RT}{\eta F}\left[\frac{1}{A_c}\left(\frac{1}{i_{o,c}} + \frac{1}{i_{L,c}}\right) + \frac{1}{A_a}\left(\frac{1}{i_{o,a}} + \frac{1}{i_{L,a}}\right)\right] + R_i$ (7)

R_t is the <u>effective</u> internal resistance of the cell.

Using (6) in (5)

$$P = I(E_r - R_t I) \tag{8}$$

The condition for maximum power is

$$dP/dI = E_r - 2R_t I_m = 0 \tag{9}$$

$$I_m = E_r/2R_t \tag{10}$$

$$P_m = E_r^2/4R_t \tag{11}$$

and

$$E_m = E_r/2 \tag{12}$$

Case (ii) Conditions under which the current-potential relation at each electrode is Tafellian.

Mass transfer and ohmic polarization are assumed to be negligible. Under these conditions the power-current relation is given by

$$P = I\left[E_r - (a_1 + a_2) - (b_1 + b_2)\log I\right] \tag{13}$$

where

$$a_1 = \frac{RT}{\alpha_c F} \ln A_c i_{o,c} \qquad b_1 = \frac{RT}{\alpha_c F} \tag{14}$$

$$a_2 = \frac{RT}{\alpha_a F} \ln A_a i_{o,a} \qquad b_2 = \frac{RT}{\alpha_a F} \tag{15}$$

For this case, the maximum power current density and terminal cell potential when the power is a maximum are given by

$$P_m = (b_1 + b_2) \exp\left(\frac{E_r - (a_1 + a_2) - (b_1 + b_2)}{b_1 + b_2}\right) \tag{16}$$

$$\log I_m = \frac{E_r - (a_1 + a_2) - (b_1 + b_2)}{b_1 + b_2} \tag{17}$$

$$E_m = (b_1 + b_2) \tag{18}$$

3. Numerical calculations showing dependence of above electrode kinetic relation on the various parameters.

Calculations have been carried out to show the dependence of the above relations on the parameters such as the exchange current densities, limiting current densities and the internal resistance of the cell. The combination of parameters, used in the calculatinns, are given in Table II and the resulting dependences of terminal cell potential, differential resistance, efficiency and power to the current are presented graphically in Fig. 1 - 4 respectively. Fig. 1.1 shows the effect of variation of Ai_1 keeping Ai_L and R_i constant for two extreme values of R_i. It is seen that there is initially a marked decrease in E and thereafter the E-I relation is linear until the limiting current, if the product Ai_o is fairly high ($\gtrsim 10^{-3}$ amp). If Ai_o is low even for one of the electrodes ($\lesssim 10^{-6}$ amp), E decreases significantly over the whole range. In Fig. 1.2, the effect of variation of Ai_L, while Ai_o and R_i are constant, is shown. The range of current is reduced by a decade for a reduction of i_L by a factor of 10. Otherwise, the shape of the curve is constant. Fig. 1.3 shows

the marked effect of the internal resistance of the cell on the linear E-I region while maintaining Ai_o and Ai_L constant. This figure shows the great importance of reducing the internal resistance of the cell. At the same time, it is also necessary to increase the exchange current densities as is seen from lines VI and VII in Fig. 1.1. The effect of activation overpotential on the differential resistance (dE/dI) - current plot (Fig. 2.1-2.3) is quite significant at low currents, whereas concentration overpotential markedly affects this plot at currents close to the limiting current. In the central region, dE/dI is nearly constant which represents the ohmic resistance.

The efficiency-current plots (Fig. 3.1-3.3) are similar to the terminal cell-potential plots (Fig. 1.1-1.3). The efficiency is a maximum when I = 0 and decreases monotonously with increasing I.

The power is plotted as a function of current in Fig. 4.1-4.3. At any particular value of I, the power is significantly increased with increase of Ai_o. P is also increased by decreasing R_i. In most of the cases calculated, except when the internal resistance of the cell is high or when Ai_o even for one of the electrodes is low, the maximum power is close to the limiting current. When the terminal cell potential-current relation is linear, the power-current plot is parabolic as expected from equation (8).

4. Summary of other work presented in paper:*

Some models of electrode design-spaghetti tube model, jet

*Details of the theoretical analysis are in the paper which will appear in the Oct. or Nov. issue of the Journal of Electroanalytical Chemistry.

electrode, porous electrode for increasing the apparent current density (and thereby reduce efficiency and power losses) were dealt with theoretically. It was concluded that the spaghetti tube model compares favorably with the best available porous electrodes and that the jet electrode model is most suitable for liquid hydrocarbons.

TABLE I

BASIC SIMILARITIES AND DISSIMILARITIES AMONG THE THREE ELECTROCHEMICAL DEVICES

Driven Cell	Fuel Cell	Secondary Battery
Cathode is negative, anode is positive	Cathode is positive anode is negative	Cathode is positive anode is negative
Reaction forced by external power source	Reaction spontaneous	Reaction spontaneous during discharge
The driving cell is tacit, inexplicit. No load. The thermodynamic potential is not important.	The load is tacit, inexplicit. The thermodynamic potential is the central point.	The load is tacit, inexplicit. The thermodynamic potential is the central point.
Accpts electricity and produces substance.	Accepts substances and produces electricity.	Accepts electricity during charging, gives out electricity during discharging.
In principle, can operate ad infinitum.	In principle, can operate ad infinitum.	Intrinsically limited to store certain amount of energy.
Can be regarded in terms of single electrodes.	Cannot be regarded in terms of single electrodes.	Cannot be regarded in terms of single electrodes.
The current which is forced through creates the polarization; current determined outside the cell. This causes certain polarization.	The potential drop at the electrode-solution interface is modified by the passage of current as a kind of feed-back. Current determined (partly) inside cell. Stimulated by $E_r - \xi_\eta$.	The potential drop at the electrode-solution interface is modified by the passage of current as a kind of feed-back.

TABLE II

KINETIC PARAMETERS USED IN THEORETICAL ANALYSIS OF PERFORMANCE OF ELECTROCHEMICAL REACTOR

Calculation number	$A_a i_{o,a}$ amps	$A_c i_{o,c}$ amps	$A_a i_{L,a}$ amps	$A_c i_{L,c}$ amps	α_a	α_c	R_i ohms
I	10^{-3}	10^{-9}	1	1	1/2	1/2	1
II	10^{-3}	10^{-3}	1	1	1/2	1/2	1
III	> 1	10^{-3}	1	1	∞	1/2	0.1
IV	10^{-3}	10^{-3}	1	1	1/2	1/2	0.1
V	> 1	10^{-3}	1	1	∞	1/2	0.01
VI	10^{-3}	10^{-3}	1	1	1/2	1/2	0.01
VII	> 1	10^{-3}	1	1	∞	1/2	0.01
VIII	10^{-3}	10^{-6}	1	1	1/2	1/2	1
IX	10^{-3}	10^{-6}	1	1	1/2	1/2	0.1
X	> 1	10^{-6}	1	1	∞	1/2	0.1
XI	> 1	10^{-3}	0.1	0.1	∞	1/2	0.01
XII	> 1	10^{-6}	0.1	0.1	∞	1/2	1

CAPTIONS TO FIGURES

1. Terminal cell potential-current plots (vide Table III for assumed kinetic parameters).

   1.1 Effect of Ai_o on E-I curves at constant values of Ai_L and R_i

   Solid lines - R_i = 1 ohm.

   Dashed lines - R_i = 0.01 ohm.

   1.2 Effect of Ai_L on E-I curves at constant values of Ai_o and R_i.

   1.3 Effect of R_i on E-I curves at constant values of Ai_o and Ai_L.

2. Differential resistance-current plots.

   Division into sub group 2.1-2.3 as in Figure 1.

3. Efficiency-current plots.

   Division into sub group as in preceding figures.

4. Power-current plots.

   Division into sub group as in preceding plots.

V

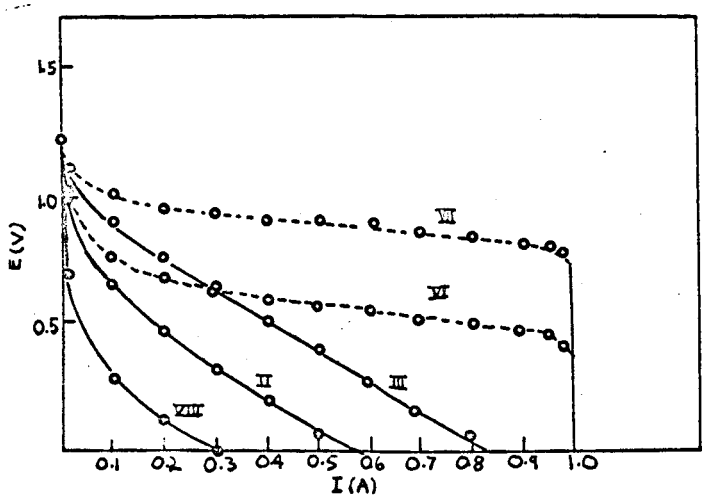
1.5
1.0
0.5
E(V)
VII
VI
III
II
VIII
0.1 0.2 0.3 0.4 0.5 0.6 0.7 0.8 0.9 1.0
I(A)

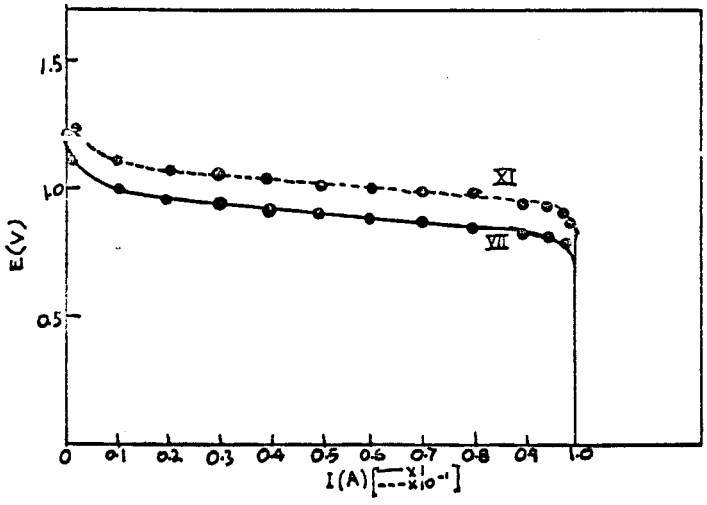
1.5
1.0
0.5
E(V)
XI
VII
0 0.1 0.2 0.3 0.4 0.5 0.6 0.7 0.8 0.9 1.0
I(A)

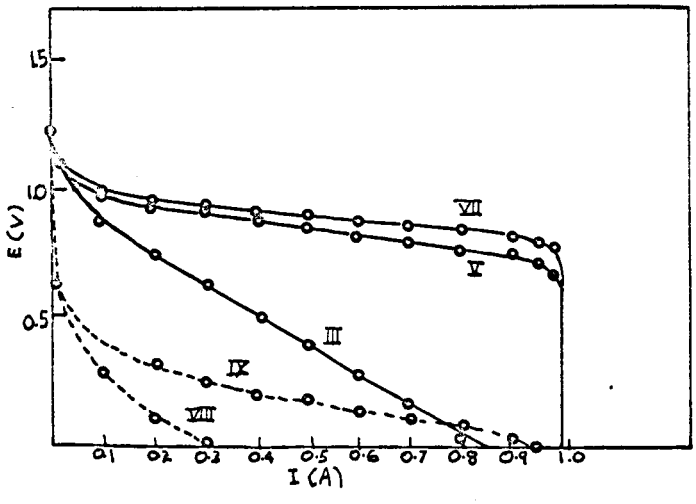
1.5
1.0
0.5
E(V)
VII
V
III
IX
VIII
0.1 0.2 0.3 0.4 0.5 0.6 0.7 0.8 0.9 1.0
I(A)

FIG. 1

V

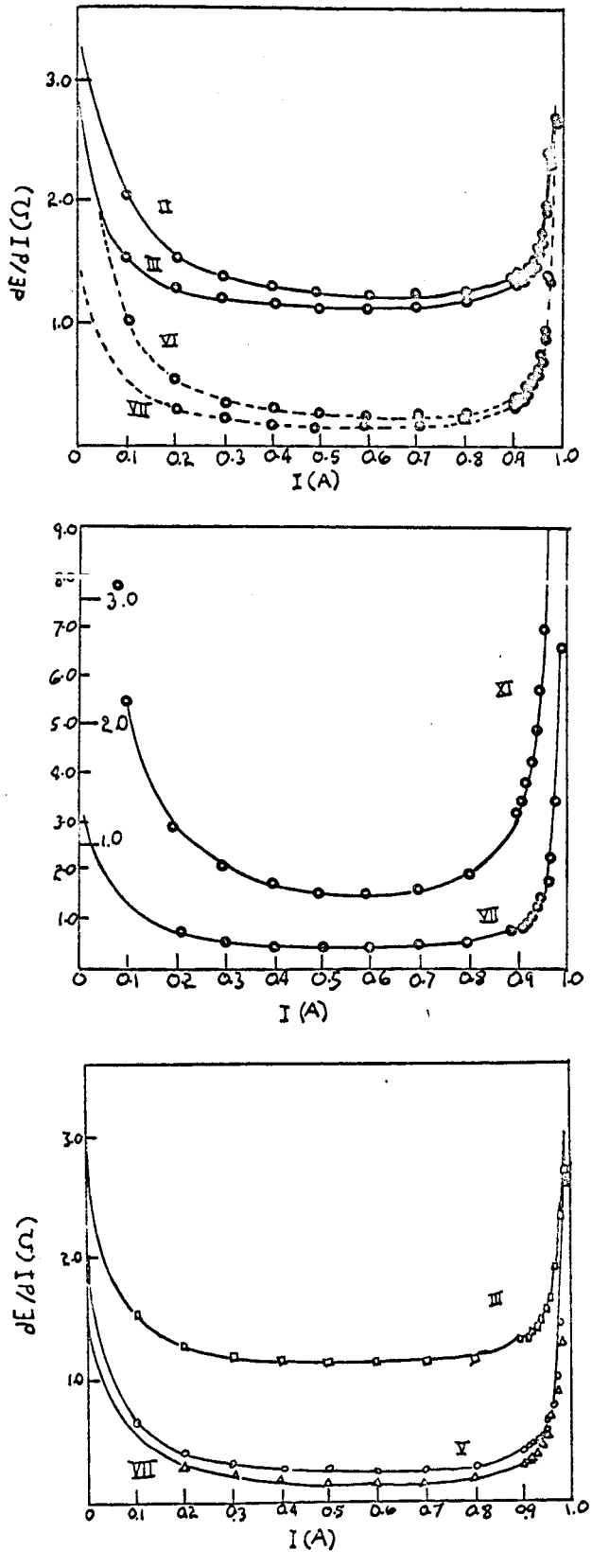

FIG.2

V

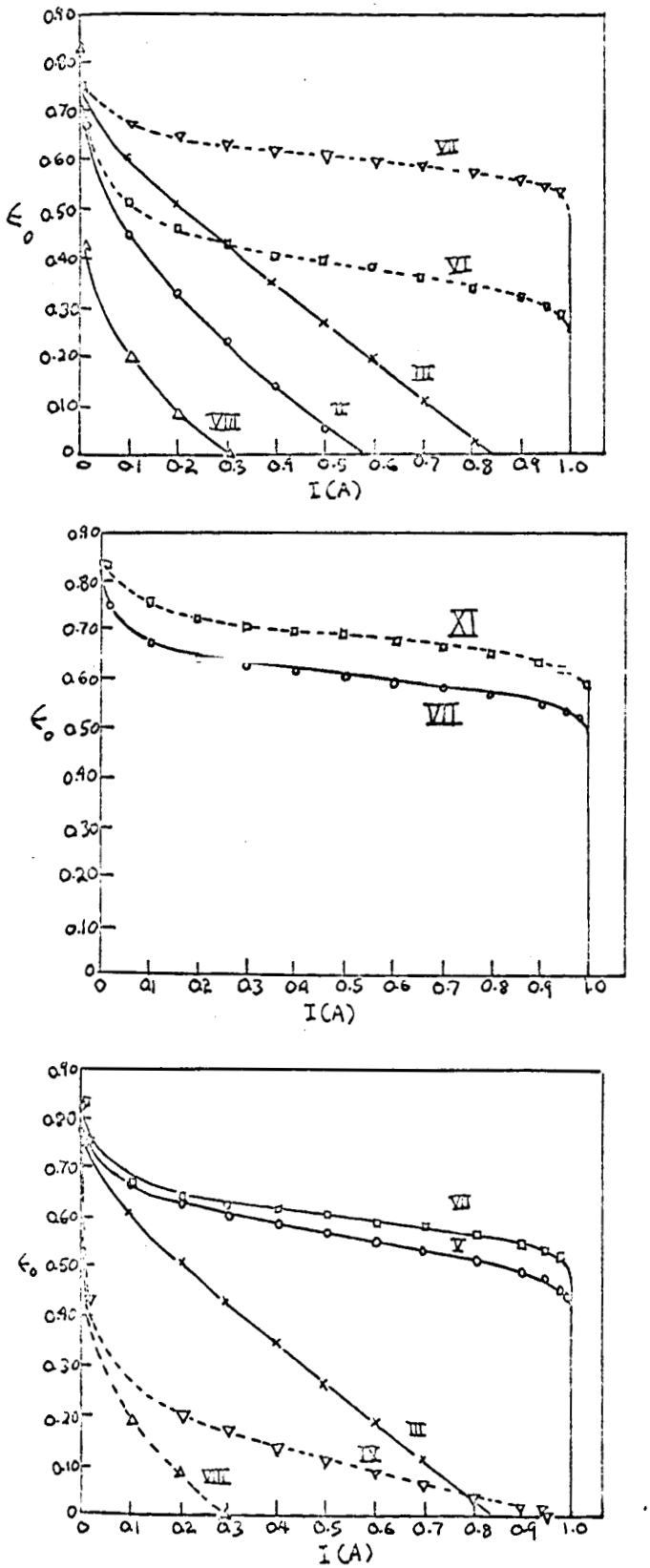

FIG. 3

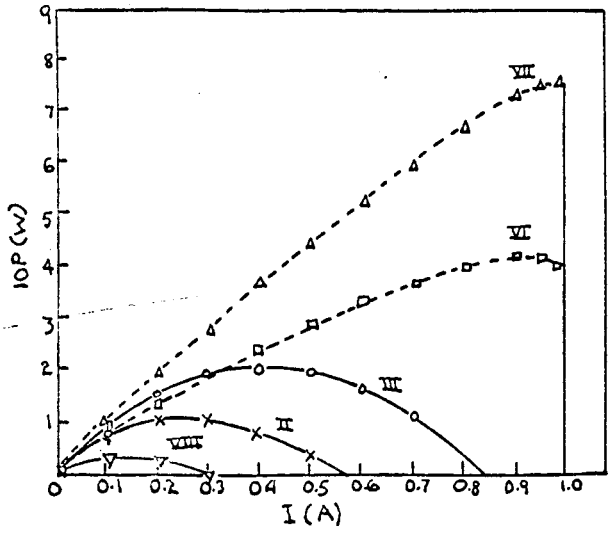
10P(w)
I(A)
VII
VI
III
II
VIII

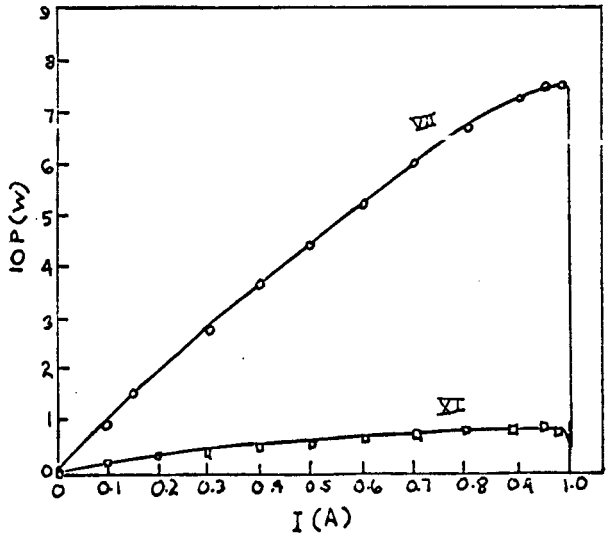
10P(w)
I(A)
VII
VI

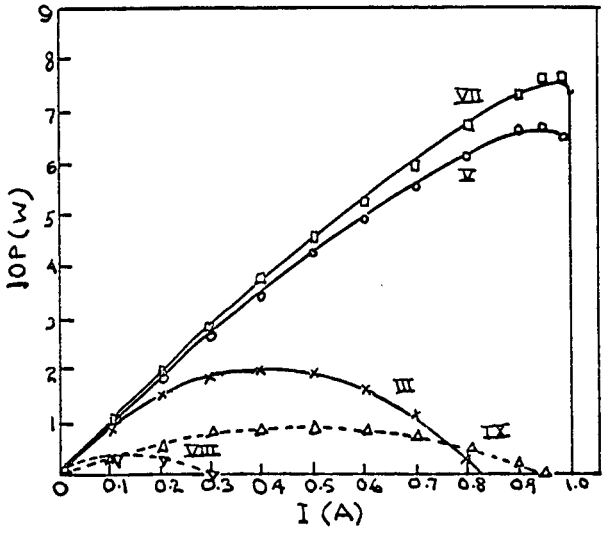
10P(w)
I(A)
VII
V
III
IX
IV
VIII

FIG. 4

VI PROJECT PERSONNEL

Section I

Mr. Boris Cahan, Pre Doctoral Research Fellow

Dr. Halina Wroblowa, Supervisor

Section II

Miss Rowshan Jahan, Pre Doctoral Research Fellow

Dr. Aleksandar Damjanovic, Supervisor

Section III

Mr. Shyam Argade, Pre Doctoral Research Fellow

Dr. Eliezer Gileadi, Supervisor

Section IV

Dr. Ljerka Duic, Post Doctoral Research Fellow

Dr. Halina Wroblowa, Supervisor

Section V

Dr. S. Srinivasan, Post Doctoral Research Fellow

Dr. John O'M. Bockris, Supervisor

VII PUBLICATIONS UNDER GRANT NsG325

1. Forces involved in the Specific Adsorption of Ions on metals from aqueous solution, J. O'M. Bockris and T. Anderson, Electrochimica Acta, 9, 347 (1964).

2. Electrochemical Kinetics of Parallel Reactions, E. Gileadi and S. Srinivasan, J. of Electroanal. Chem., 7 (1964) 452-457.

3. Electrocatalysis, J. O'M. Bockris and H. Wroblowa, J. Electroanal Chem., 7 (1964) 428-451.

4. Basis of possible continuous self activation in an electrochemical energy converter, J. O'M. Bockris, B. J. Piersma, E. Gileadi and D. D. Cahan, J. Electroanal. Chem., 7 (1964) 487-490.

5. Ellipsometry in Electrochemical Studies, A. K. N. Reddy and J. O'M. Bockris, U.S. Dept. Comm. Natl. Bureau of Standards, Mics Publication 256, Sept. 15, 1964, 229-244.

6. Ellipsometric Study of oxygen-containing films on Platinum electrodes. A. K. N. Reddy, M. Genshaw and J. O'M. Bockris, J. Electroanal. Chem., 8 (1964) 406-407.

7. Ellipsometric Determination of the Film Thickness and Conductivity during the Passivation Process on Nickel, A. K. N. Reddy, M. G. B. Rao and J. O'M. Bockris, J. Chem. Phys., 42, 6, 2246-2248, 15 March 1965.

8. A Brief Outline of Electrocatalysis, J. O'M. Bockris and S. Srinivasan, 19th Annual Proceedings Power Sources Conference, May 1965.

The Following are in course of publication.

9. Potential of Zero Charge, S. D. Argade and E. Gileadi.

10. The Potential Sweep Method: A Theoretical Analysis, S. Srinivasan and E. Gileadi.

11. Proton Transfer across Double Layers, J. O'M. Bockris, S. Srinivasan and D. B. Matthews.

12. An ellipsometric study of oxide films on platinum in acid solutions, J. O'M. Bockris, A. K. N. Reddy and M. Genshaw.

13. Electrode Kinetic Aspects of Elect.chemical Energy Conversion, J. O'M. Bockris and S. Srinivasan.

VIII DISTRIBUTION LIST FOR FUEL CELL REPORTS

National Aeronautics & Space Administration
Washington, D.C. 20546
Attn: Ernst M. Cohn, Code RNW
George F. Esenwein, Code MAT
A. M. Andrus, Code ST
J. R. Miles, Code SL

National Aeronautics & Space Administration
Scientific and Technical Information Facility
P.O. Box 5700
Bethesda, Maryland, 20014 (3)

National Aeronautics & Space Administration
Goddard Space Flight Center
Greenbelt, Maryland
Attn: Thomas Hennigan

National Aeronautics & Space Administration
Langley Research Center
Langley Station
Hampton, Virginia
Attn: S. T. Peterson

National Aeronautics & Space Administration
Lewis Research Center
21000 Brookpark Road
Cleveland 35, Ohio
Attn: N. D. Sanders
Robert Miller
Robert L. Cummings

National Aeronautics & Space Administration
Marshall Space Flight Center
Huntsville, Alabama
Attn: Philip Youngblood

National Aeronautics & Space Administration
Ames Research Center
Pioneer Project
Moffett Field, California
Attn: James R. Swain

Cell Reports (con't.)

National Aeronautics & Space Administration
Manned Spacecraft Center
Houston 1, Texas
Attn: Richard Ferguson (for EP-5)
Robert Cohen
Forrest E. Eastman, EE-4

National Aeronautics & Space Administration
Ames Research Center
Mountain View, California
Attn: Jon Rubenzer, Biosatellite Project

Jet Propulsion Laboratory
4800 Oak Grove Drive
Pasadena, California
Attn: Aiji Uchiyama

DEPARTMENT OF THE ARMY

U.S. Army Engineer R&D Labs.
Fort Belvoir, Virginia
Attn: Electrical Power Branch

U.S. Army Engineer R&D Labs.
Fort Monmouth, New Jersey
Attn: Arthur F. Daniel (Code SELRA/SL-PS)

U.S. Army R&D Liaison Group (9851 DV)
APO 757
New York, New York
Attn: Chief, Chemistry Branch

U.S. Army Research Office
Physical Sciences Division
3045 Columbia Pike
Arlington, Virginia

Harry Diamond Labs.
Room 300, Building 92
Connecticut Avenue & Van Ness Street, N.W.
Washington, D.C.
Attn: Nathan Kaplan

Cell Reports (con't.)

Army Material Command
Research Division
AMCRD-RSCM T-7
Washington 25, D.C.
Attn: John W. Crellin

Natick Labs.
Clothing & Organic Materials Div.
Natick, Massachusetts
Attn: Leo A. Spano/Robert N. Walsh

U.S. Army TRECOM
Physical Sciences Group
Fort Eustis, Virginia
Attn: (SMOPE)

U.S. Army Research Office
Box CM, Duke Station
Durham, North Carolina
Attn: Paul Greer/Dr. Wilhelm Jorgensen

U.S. Army Mobility Command
Research Division
Center Line, Michigan
Attn: O. Renius (AMSMO-RR)

Hq., U.S. Army Material Command
Development Division
Washington 25, D.C.
Attn: Marshall D. Aiken (AMCRD-DE-MO-P)

DEPARTMENT OF THE NAVY

Office of Naval Research
Department of the Navy
Washington 25, D.C.
Attn: Dr. Ralph Roberts/H.W. Fox

Cell Reports (con't)

Mr. J. H. Harrison
Special Projects Division
U.S. Navy Marine Engineering Lab.
Annapolis, Maryland 21402

Bureau of Naval Weapons
Department of the Navy
Washington 25, D.C.
Attn: (Code RAAE)

U.S. Naval Research Laboratory
Washington, D.C., 20390
Attn: (Code 6160)

Bureau of Ships
Department of the Navy
Washington 25, D.C.
Attn: Bernard B. Rosenbaum/C. F. Viglotti

Naval Ordance Laboratory
Department of the Navy
Corona, California
Attn: Mr. William C. Spindler (Code 441)

Naval Ordance Laboratory
Department of the Navy
Silver Spring, Maryland
Attn: Philip B. Cole (Code WB)

DEPARTMENT OF THE AIR FORCE

Wright-Patterson AFB
Aeronautical Systems Division
Dayton, Ohio
Attn: George W. Sherman, APIP

AF Cambridge Research Lab
Attn: CRZE
L. G. Hanscom Field
Bedford, Massachusetts
Attn: Francis X. Doherty/Edward Raskind (Wing F)

Cell Reports (cont'd.)

Rome Air Development Center, ESD
Griffiss AFB, New York
Attn: Frank J. Mollura (RASSM)

Space Systems Division
Attn: SSZAE-11
Air Force Unit Post Office
Los Angeles 45, California

Air Force Ballistic Missile Division
Attn: WEZYA-21
Air Force Unit Post Office
Los Angeles 45, California

ATOMIC ENERGY COMMISSION

Mr. Donald B. Hoatson
Army Reactors, DRD
U.S. Atomic Energy Commission
Washington 25, D.C.

OTHER GOVERNMENT AGENCIES

Office, DDR&E: USW & BSS
The Pentagon
Washington 25, D.C.
Attn: G. B. Wareham

Mr. Kenneth B. Higbie
Staff Metallurgist
Office, Director of Metallurgy Research
Bureau of Mines
Interior Building
Washington, D.C., 20240

Institute for Defense Analyses
Research and Engineering Support Division
400 Army-Navy Drive
Arlington, Virginia 22202
Attn: Dr. George C. Szego/R. Hamilton

Cell Reports (cont'd.)

Power Information Center
University of Pennsylvania
Moore School Building
200 South 33rd Street
Philadelphia 4, Pennsylvania

Chief, Input Section, CFSTI
Sills Building
5285 Port Royal Road
Springfield, Virginia, 22151

PRIVATE INDUSTRY

Alfred University
Alfred, New York
Attn: Professor T. J. Gray

Allis-Chalmers Mfg. Co.
1100 S. 70th Street
Milwaukee 1, Wisconsin
Attn: Dr. W. Mitchell, Jr.

Allison Division of General Motors
Indianapolis 6, Indiana
Attn: Dr. Robert E. Henderson

American Cyanamid Company
1937 W. Main Street
Stamford, Connecticut
Attn: Dr. R. G. Haldeman

American Machine & Foundry
689 Hope Street
Springdale, Connecticut
Attn: Dr. L. H. Shaffer
Research & Development Division

Cell Reports (cont'd.)

Astropower, Inc.
2968 Randolph Avenue
Costa Mesa, California
Attn: Dr. Carl Berger

Battelle Memorial Institute
Columbus 1, Ohio
Attn: Dr. C. L. Faust

Bell Telephone Laboratories, Inc.
Murray Hill, New Jersey
Attn: Mr. U. B. Thomas

Clevite Corporation
Mechanical Research Division
540 East 105th Street
Cleveland, Ohio
Attn: A. D. Schwope

Electrochimica Corp.
1140 O'Brien Drive
Menlo Park, California
Attn: Dr. Morris Eisenberg

Electro-Optical Systems, Inc.
300 North Halstead Street
Pasadena, California
Attn: E. Findl

Engelhard Industried, Inc.
497 DeLancy Street
Newark 5, New Jersey
Attn: Dr. J. G. Cohn

Esso Research and Engineering Company
Products Research Division
P.O. Box 215
Linden, New Jersey
Attn: Dr. Carl Heath

Cell Reports (cont'd.)

The Franklin Institute
Philadelphia, Pennsylvania
Attn: Mr. Robert Goodman

General Electric Company
Direct Energy Conversion Operations
Lynn, Massachusetts
Attn: Dr. E. Glazier

Garrett Corp.
1625 Eye St., N.W.
Washington 6, D.C.
Attn: George R. Shepherd

General Electric Company
Research Laboratory
Schenectady, New York
Attn: Dr. H. Liebhafsky

General Electrid Company
Missile and Space Division (Room M1330)
P.O. Box 8555
Philadelphia 1, Pennsylvania
Attn: L. Chasen

General Motors Corp.
Box T
Santa Barbara, California
Attn: Dr. C. R. Russell

Globe-Union, Inc.
Milwaukee 1, Wisconsin
Attn: Dr. C. K. Morehouse

Dr. Joseph S. Smatko
General Motors
Defense Research Laboratories
P.O. Box T
Santa Barbara, California, 93102

Cell Reports (cont'd.)

John Hopkins University
Applied Physics Laboratory
8621 Georgia Avenue
Silver Spring, Maryland
Attn: W. A. Tynan

Leesona Moos Laboratories
Lake Success Park
Community Drive
Great Neck, New York
Attn: Dr. A. Moos

McDonnell Aircraft Corporation
Attn: Project Gemini Office
P.O. Box 516
St. Louis 66, Missouri

Monsanto Research Corporation
Everette 49, Massachusetts
Attn: Dr. J. O. Smith

North American Aviation Co.
S&ID Division
Downey, California
Attn: Dr. James Nash

Pratt and Whitney Aircraft Division
United Aircraft Corporation
East Hartford 8, Connecticut
Attn: Librarian

Radio Corporation of America
Astro Division
Heightstown, New Jersey
Dr. Seymour Winkler

Radio Corporation of America
Somerville, New Jersey
Attn: Dr. G. Lozier

Cell Reports (cont'd.)

Speer Carbon Company
Research and Development Laboratories
Packard Road at 47th Street
Niagara Falls, New York
Attn: Dr. L. M. Liggett

Stanford Research Institute
820 Mission Street
So. Pasadena, California
Attn: Dr. Fritz Kalhammer

Thiokol Chemical Corporation
Reaction Motors Division
Denville, New Jersey
Attn: Dr. D. J. Mann

Thompson Ramo Wooldridge
2355 Euclid Avenue
Cleveland 17, Ohio
Attn: Mr. Victor Kovacik

Unified Science Associates, Inc.
826 S. Arroyo Parkway
Pasadena, California
Attn: Dr. Sam Naiditch

Union Carbide Corporation
12900 Snow Road
Parma, Ohio
Attn: Dr. George E. Evans

University of California
Space Science Laboratory
Berkeley 4,California
Attn: Prof. Charles W. Tobias

University of Pennsylvania
Philadelphia 4, Pennsylvania
Attn: Dr. Manfred Altman

Cell Reports (cont'd.)

Western Reserve University
Cleveland, Ohio
Attn: Prof. Ernest Yeager

Yardney Electric Corp.
New York, New York
Attn: Dr. Paul Howard

Lockheed Missiles & Space Co.
3251 Hanover St.
Palo Alto, California
Attn: Dr. George B. Adams

Mr. B. S. Baker
Institute of Gas Technology
State & 34th Streets
Chicago 16, Illinois

Mr. Peter D. Richman
President
Chem Cell Inc.
3 Central Ave.
East Newark, New Jersey 07029